NASA TECHNICAL NOTE

NASA TN D-7031

AERODYNAMIC CHARACTERISTICS OF A LARGE-SCALE MODEL WITH A LIFT FAN MOUNTED IN A 5-PERCENT-THICK TRIANGULAR WING, INCLUDING THE EFFECTS OF BLC ON THE LIFT-FAN INLET

by Brent K. Hodder, Jerry V. Kirk, and Leo P. Hall

Ames Research Center
and
U. S. Army Air Mobility R & D Laboratory
Moffett Field, Calif. 94035

NATIONAL AERONAUTICS AND SPACE ADMINISTRATION • WASHINGTON, D. C. • DECEMBER 1970

1. Report No.	2. Government Accession No.	3. Recipient's Catalog No.
NASA TN D-7031		

4. Title and Subtitle
AERODYNAMIC CHARACTERISTICS OF A LARGE-SCALE MODEL WITH A LIFT FAN MOUNTED IN A 5-PERCENT-THICK TRIANGULAR WING, INCLUDING THE EFFECTS OF BLC ON THE LIFT-FAN INLET

5. Report Date: December 1970

6. Performing Organization Code:

7. Author(s)
Brent K. Hodder, Jerry V. Kirk, and Leo P. Hall

8. Performing Organization Report No.: A-2822

9. Performing Organization Name and Address
NASA Ames Research Center
and
U.S. Army Air Mobility R & D Laboratory
Moffett Field, Calif., 94035

10. Work Unit No.: 721-01-00-05-00-21

11. Contract or Grant No.:

12. Sponsoring Agency Name and Address
National Aeronautics and Space Administration
Washington, D. C., 20546

13. Type of Report and Period Covered: Technical Note

14. Sponsoring Agency Code:

15. Supplementary Notes

16. Abstract

The low-speed aerodynamics of a large-scale triangular wing model, with a reduced thickness, tip-turbine driven lift fan in each wing were investigated in the Ames 40- by 80-Foot Wind Tunnel. The model had a 5-percent-thick wing typical of wings designed for supersonic performance. Conventional lift-fan depth has, in the past, limited wing thickness to about 10 percent. A thinner lift fan for the present investigation was obtained by modification of a conventional fan. The modification included removing the discharge stator and reducing the fan inlet length and radius. To control airflow separation resulting from small inlet radii, blowing boundary-layer control was applied through a nozzle in the inlet.

Performance of the modified fan along with aerodynamic characteristics of the total configuration is presented. The static thrust performance of the conventional fan (requiring a 10-percent wing) was equalled by the reduced thickness fans of this investigation.

17. Key Words (Suggested by Author(s))
Fan and wing model
Lift-fan 5 degree triangular wing
Lift-fan with boundary layer control

18. Distribution Statement
Unclassified-Unlimited

19. Security Classif. (of this report)	20. Security Classif. (of this page)	21. No. of Pages	22. Price*
Unclassified	Unclassified	52	$3.00

*For sale by the National Technical Information Service, Springfield, Virginia 22151

NOTATION

A	wing aspect ratio
A_d	fan disk area, sq ft
A_f	fan annulus area (excluding tip-turbine area), sq ft
a	lift-curve slope, $\frac{\partial C_L}{\partial \alpha}$
b	wing span, ft
c	wing chord parallel to plane of symmetry, ft
$\bar{c}$	mean aerodynamic chord, $\frac{2}{S} \int_0^{b/2} c^2 \, dy$, ft
C_D	drag coefficient, $\frac{D}{q_\infty S}$
C_L	lift coefficient, $\frac{L}{q_\infty S}$
C_m	pitching-moment coefficient, $\frac{M}{q_\infty S \bar{c}}$
C_{μ_f}	blowing momentum coefficient, $\frac{W/g}{2A_f q_{f_{BLC\ off}}} V_j$
D	drag, lb
D_F	diameter of fan, ft
g	acceleration of gravity, 32.2 ft/sec^2
L	total lift of model, lb
M	pitching moment, ft-lb
p_t	total pressure, lb/sq ft
p_s	static pressure, lb/sq ft
q	dynamic pressure, lb/sq ft
R	fan radius, ft
rpm	fan rotational speed corrected to standard-day conditions
S	projected wing area, sq ft

T	lift-fan thrust perpendicular to wing chord plane with $\beta_v = 0°$, $\alpha = 0°$, $T = 2A_f q_f$, lb
T_t	total temperature, °F
V	air velocity, ft/sec unless otherwise noted
V_f	lift-fan discharge velocity, ft/sec
W	weight rate of flow of BLC air, lb/sec
α	angle of attack of the wing chord plane, deg
β_v	fan exit-vane deflection angle from the fan vertical axis, deg
δ_F	trailing-edge flap deflection measured normal to hinge line, deg
μ	tip-speed ratio, $\frac{V_\infty}{\omega R}$
ρ	mass density of air, slugs/cu ft
ω	fan rotational speed, radians/sec

Subscripts

j	BLC blowing jet
∞	free stream
s	static condition, $q_\infty = 0$
po	power off
BLC on	boundary-layer control applied
BLC off	boundary-layer control not applied

AERODYNAMIC CHARACTERISTICS OF A LARGE-SCALE MODEL WITH A LIFT FAN MOUNTED IN A 5-PERCENT-THICK TRIANGULAR WING, INCLUDING THE EFFECTS OF BLC ON THE LIFT-FAN INLET

Brent K. Hodder, Jerry V. Kirk, and Leo P. Hall

Ames Research Center
and
U.S. Army Air Mobility R & D Laboratory

SUMMARY

The low-speed aerodynamics of a large-scale triangular wing model, with a reduced thickness, tip-turbine driven lift fan in each wing were investigated in the Ames 40- by 80-Foot Wind Tunnel. The model had a 5-percent-thick wing typical of wings designed for supersonic performance. Conventional lift-fan depth has, in the past, limited wing thickness to about 10 percent. A thinner lift fan for the present investigation was obtained by modification of a conventional fan. The modification included removing the discharge stator and reducing the fan inlet length and radius. To control airflow separation resulting from small inlet radii, blowing boundary-layer control was applied through a nozzle in the inlet.

Performance of the modified fan along with aerodynamic characteristics of the total configuration is presented. The static thrust performance of the conventional fan (requiring a 10-percent wing) was equalled by the reduced thickness fans of this investigation.

INTRODUCTION

Previous wind-tunnel investigations (refs. 1, 2, 3) of V/STOL fan-in-wing concepts have been limited to subsonic aircraft configurations because of the wing thickness required to house the fan dictated subsonic cruise performance. In the interest of applying the fan-in-wing concept to supersonic configurations, this investigation endeavored to reduce the fan thickness for installation in a 5-percent wing. To reduce fan thickness, the discharge stator was removed, inlet length and radius were reduced, and boundary-layer control was added. (Other means of minimizing fan thickness are discussed in reference 4, but the methods require total redesign of the fan and exceeded the scope of this investigation.) A triangular wing planform was chosen to maximize absolute wing thickness while minimizing the dimensionless wing thickness.

Aerodynamic force and pitching-moment characteristics of the model are presented and limited comparisons are made between these results and those from other lift-fan V/STOL aircraft configurations. Effects of boundary-layer

control on fan performance with and without forward speed are presented and performance of the reduced thickness fan is compared with that of the conventional fan.

MODEL AND APPARATUS

Aircraft

The model is shown in figure 1 mounted on the normal strut system in the Ames 40- by 80-Foot Wind Tunnel. Figure 2 is a close-up photograph of the reduced thickness lift fan. Note that the contoured BLC inlet was installed only on the outboard side of the fan where the wing was too thin to accommodate the full thickness of the conventional fan inlet. Figure 3 is a sketch of the model showing pertinent dimensions.

Wing geometry- The mid-mounted wing had an aspect ratio of 2.30 and a leading-edge sweep of 60°. An NACA 16-005 (modified) airfoil section (coordinates in table 1) was basic for the wing.

The wing had a single-slotted trailing-edge flap which extended from 14.1- to 73.4-percent semispan. Provisions were made for 0°, 30°, and 60° flap deflections.

Fuselage- The fuselage was slab sided with rounded corners and was approximately 4 feet wide. Two YJ-85-5 turbojet engines were mounted side by side high on the fuselage.

Tail- Figure 3 shows the location and details of the vertical tail. All results shown are with the horizontal tail off.

Propulsion System

The X-353-5B lift fan has been thoroughly described in previous investigations (refs. 1, 2, and 5). The wing fans are tip-turbine driven by exhaust gases from the YJ-85-5 jet engines. Both fans rotated in a counterclockwise direction when viewed from above the model.

Lift-fan installation- Location of the wing mounted lift fans is shown in figure 3. The fans were completely enclosed within the wing with the exception of the fan hub which, because of mechanical complexity, was not modified to fall within the wing contour. However, it is felt that proper hub modification would not invalidate fan performance presented in this investigation. Tee-shaped diverter valves mounted behind the jet engines were used to divert exhaust gases to power the lift fans or to provide forward thrust. A cascade of exit vanes was mounted directly beneath each fan (see fig. 4) to vector the fan exhaust. The exit vane airfoil section had a chord of 14 inches, a maximum thickness of 10-percent chord at 20-percent chord, and

a maximum camber of 3.6-percent chord at 35-percent chord. The exit vane cascade spanned the fan rotor and tip-turbine discharge. Thrust vectoring was accomplished by symmetrical actuation of the exit vanes.

Lift-fan inlet modification- The fan inlet was modified as shown in figure 5. Essentially, the conventional bellmouth inlet and circular inlet guide vane were removed from the outboard 180° of the fan. This inlet section was then replaced by an inlet of varying radius which would blend in with the local contours of the wing. A blowing nozzle for boundary-layer control was incorporated in the inlet.

Boundary-layer-control system and measurement- Two 300-horsepower electric motors powered a centrifugal flow compressor to provide the boundary-layer-control air. Compressor discharge was exhausted to the semicircular plenum chamber ahead of the nozzle for each inlet. Two nozzle geometries were tested as shown in figure 6. Total and static pressure and total temperature measurements were made at station 1 (see fig. 6) for determination of BLC air mass flow. Nozzle velocity was computed from total pressure measurements at station 2 (fig. 6) assuming isentropic expansion. Nozzle gap was set at 0.040 inch for the entire investigation.

Fan thrust measurement- Zero-forward-speed thrust of both lift fans was obtained from the wind-tunnel force balance while fan thrust with forward speed was derived from total pressure rakes mounted directly beneath each fan.

TESTING PROCEDURE

Longitudinal force and moment data were obtained for angles of attack from -4° to +24°. Tunnel airspeed was varied from 0 to 100 knots corresponding to a maximum Reynolds number of 17.8 million. Fan speed was varied from 1100 to 1700 rpm; however, for the majority of the investigation fan speed was held at approximately 1700 rpm.

Tests at Zero Angle of Attack

At zero angle of attack, fan speed, BLC momentum, wind-tunnel velocity, and exit vane angle were varied independently. Data were obtained for both BLC nozzles, exit vanes on and off, and three flap deflections.

Tests at Variable Angle of Attack

When angle of attack was varied, fan rpm and BLC momentum were held essentially constant. Results were obtained for several tunnel airspeeds with and without BLC, exit vanes on and off, and three flap deflections. Power-off runs were made with fan inlets sealed and exit vanes closed.

CORRECTIONS

Force data obtained with the fans not operating (power off) were corrected for the effects of wind-tunnel wall interference in the following manner:

$$\alpha = \alpha_u + 0.8120\ C_{L_u}$$

$$C_D = C_{D_u} + 0.0142\ C_{L_u}$$

A ΔC_D correction was applied to all data to account for tares resulting from exposed tips on the strut mounting system. Additional ΔC_D and ΔC_m corrections were applied to all longitudinal results to adjust for an unfaired tail strut.

Reference 3 presents criteria for acceptable boundaries of model to wind-tunnel size ratios that are known to give negligible wall effects. This information is based on comparison of wind-tunnel and flight-test data. For models having concentrated lifting elements, such as lift fans, the most important parameter is probably the lifting element ratio. The model of this investigation had a lifting element area ratio and disk loading within the boundaries presented in reference 3. Therefore, no wind-tunnel wall corrections have been applied to the results with the lift fans operating.

RESULTS

The relationship between fan tip-speed ratio and free stream to fan velocity ratio is presented in figure 7. For convenience, lift-fan tip-speed ratio is used as the independent parameter for the presentation of results unless otherwise stated.

Table 2 is an index to the basic data figures. The first section of the table is devoted to lift-fan performance data only; the second section to model longitudinal force and moment data at zero angle of attack with lift-fans operating; and the third section to the variation of longitudinal results with angle of attack.

Lift-Fan Characteristics

Zero airspeed- Lift-fan static thrust for all configurations tested is shown in figure 8. Data were obtained with and without BLC applied ($C_{\mu_f} = 0.025$ and $C_{\mu_f} = 0$, respectively), exit vane cascades on and off, and for two BLC jet nozzles. When BLC was applied, blowing momentum was held essentially constant as rpm was varied.

Variable airspeed- Fan thrust variation with forward speed, derived from fan exit total pressure measurements, is shown with and without BLC in figure 9. In both cases the exit vane cascade was installed and in the 0° position.

Longitudinal Characteristics

Zero angle of attack- Lift, drag, and pitching-moment coefficients at zero angle of attack are presented in figures 10(a) to 10(i) for exit vane deflections of 0° to 50° at flap deflections of 0°, 30°, and 60°. All data are for lift-fans operating and BLC applied to the fan inlet, except figures 10(f) and 10(g), which provide BLC off data for comparison at the 30° flap deflection. In figures 10(a) to 10(i), lift coefficient is plotted on a logarithmic scale for better accuracy.

Variable angle of attack- Longitudinal aerodynamic characteristics at variable angle of attack are presented in figures 11 to 13(d) for airspeeds from 30 to 100 knots with flap deflections of 0°, 30°, and 60°. Power-off characteristics (fig. 11) were obtained with fan inlet cavities covered and exit vanes in the fully closed position. Power-on characteristics (figs. 12(a) to 13(d)) with and without BLC are compared at each forward speed but only for the 30° flap deflection. The data for all other flap deflections are for BLC applied. The exit vanes were set to give thrust (horizontal direction) equal to drag at zero angle of attack. In addition, power-on characteristics were obtained with the exit vane cascade removed. Forces and moments obtained at low tunnel airspeeds have been made dimensionless by fan static thrust.

DISCUSSION

Lift-Fan Performance

BLC effects at zero airspeed- Boundary-layer control applied to the fan inlet substantially increased fan thrust (fig. 8), indicating a reduction of inlet flow separation and subsequent improvement in total pressure recovery. Exit total pressure measurements (fig. 14) show a large increase in total pressure due to BLC at the blade tip with a smaller increase over the remainder of the blade up to the hub. An additional induced effect due to BLC is evidenced by an increase in total pressure on the inboard side of the fan rotor with the conventional inlet. Fan thrust was improved more with a 120° BLC nozzle than with a 90° nozzle, which evidently caused poor jet attachment on the fan inlet and is therefore only documented in figure 8. Figure 8 shows that inserting the exit vane cascade increased fan thrust significantly when BLC was not applied; but with BLC, the cascade insertion caused only a small thrust increase. This suggests that with the increase in fan loading due to BLC, the accompanying increase in fan efflux swirl angle causes relatively large losses in the cascade. When BLC is off, fan loading and swirl angle are reduced, allowing the cascade to turn the swirl velocity to the axial direction more efficiently, but with the overall thrust level lower than with BLC.

The following comment should be made, however, regarding the subject of the fan thrust increase achieved with BLC. BLC in this type application is probably effective only when a limiting inlet depth to diameter ratio is not exceeded. An exploratory investigation at Ames indicated that BLC could be ineffective in a deeper duct.

To gage the effectiveness of the reduced thickness fan with BLC, its lift generating capability was compared with that of a conventional fan (ref. 1) (fig. 15). The conventional fan was designed with an inlet radius equal to 6 percent of the fan rotor diameter, a circular inlet guide vane, and a discharge stator. The lift of the conventional and reduced thickness fans was equal over the rpm range tested. However, the thrust of the BLC fan should be lower than that of the conventional fan for the same total gas horsepower input due to that portion required for BLC air. Unfortunately, direct measurement of gas horsepower was not available from reference 1, but by making use of the compressor map supplied by the engine manufacturer, it was possible to estimate a gas horsepower trend. Figure 16 shows lift versus fan rpm for the modified fan with and without BLC. The dashed lines are lines of constant turbine gas horsepower supplied to the system. For dashed line (1), the system is comprised of only the fans. For dashed line (2), the system includes the fan and BLC apparatus if used. The effect on fan lift of providing power for BLC air is shown by the loss in lift from the intersection of the lift curve (BLC on) with constant power curve (1) to constant power curve (2). Following the total system power curve (2) shows that lift with BLC is higher than lift without BLC; thus BLC provided net improvement.

The effects of varying BLC momentum on fan thrust are shown in figure 17. The ratio of lift with BLC to lift without BLC is plotted as a function of BLC momentum coefficient C_{μ_f}. The coefficient C_{μ_f} relates BLC jet momentum to fan exit momentum. Classic momentum coefficients have related a jet velocity to an adjacent velocity into which the jet exhausts. In the present case this would require a difficult measurement of the fan inlet velocity near the BLC nozzle; therefore, the fan exit velocity, an easier quantity to measure and proportional to inlet local velocity, was used instead. As with curves of lift coefficient versus blowing coefficients for a wing flap, there is a relatively large variation of lift with C_{μ_f} until flow attachment occurs, and then increased blowing indicates that most of the gain from BLC is realized when $C_{\mu_f} = 0.025$. The effect of varying fan rpm on the correlation of lift with C_{μ_f} appears to be small. A nominal value of $C_{\mu_f} = 0.025$ was used during the investigation of basic model aerodynamic characteristics.

Lift-fan exhaust vectoring- Fan discharge vectoring by the exit vane cascade is shown in figure 18 along with comparative data for the conventional lift fan of reference 5. Chord-to-pitch ratio for the present cascade was 1.37 and 1.40 for reference 5 data, but vane aspect ratio was half that used in reference 5. In both cases the exit vane airfoil section characteristics were the same. Reference 5 data indicate efficient vectoring up to 30° while the present cascade is only efficient to approximately 12°. The loss of vectoring capability with the reduced thickness fan is probably due to either

exhaust swirl separating the exit vane cascade airflow prematurely or more pronounced end effects with the low-aspect-ratio louvers.

BLC effects at forward speed- The effects of variable BLC momentum on fan performance was again examined with the added influence of forward speed. The momentum coefficient C_{μ_f} was used again. However, in order to collapse data at each forward speed into a single curve the final momentum coefficient took the form $C_{\mu_f}(V_{f_{BLC\ off}}/V_\infty)$. Total model lift ratio is plotted in figure 19 versus the momentum coefficient $C_{\mu_f}(V_{f_{BLC\ off}}/V_\infty)$. For a more complete look at BLC effects, total model lift ratio was used because of the large influence of fan performance on wing lift. The momentum parameter $C_{\mu_f}(V_{f_{BLC\ off}}/V_\infty)$, which now contains all the principle velocities interacting near the BLC nozzle, can be interpreted as the BLC to fan momentum ratio times the tangent of the flow angle through the fan or as the ratio of BLC momentum to fan ram drag. The effect of varying fan rpm on the correlation of lift with $C_{\mu_f}(V_{f_{BLC\ off}}/V_\infty)$ is shown to be small (fig. 20).

Thrust variation with forward speed- The variation of fan-thrust-to-static-thrust ratio (at constant fan rpm) with forward speed (fig. 9) shows that on a dimensionless basis BLC had little effect on fan performance at forward speed. On an absolute basis, however, lift with BLC was considerably larger than without BLC (fig. 8). In comparison with the conventional lift-fan (fig. 21), the modified fan improved the thrust ratio at tip-speed ratios greater than 0.06. Since dimensionless performance with forward speed of the modified fans, with or without BLC, was better than that of the conventional fan, flow separation may have occurred in the conventional fan discharge stator.

Longitudinal Characteristics of the Model

Zero angle of attack- Figure 22 shows that variation of lift with airspeed with and without the flaps deflected. Measured total lift and the sum of fan thrust plus power-off lift are presented. The difference between total lift and the sum of fan thrust plus power off lift is the induced lift. Comparison of the data with flaps up and down reveals that induced lift with the flaps deflected 30° is 28 percent (at $V_\infty/V_{f_{BLC\ on}} = 0.4$) less than with the flaps up. This loss is slightly more than half the loss reported in reference 7 where a somewhat larger portion of the flap was located behind the fans. The effects on lift of a fan operating ahead of a flap are not fully understood because of the complex nature of the flow field.

Concerning the magnitude of lift induced by fan operation, reference 6 gives some insight into the more important variables that affect induced lift. Data from various wind-tunnel models are presented to show effects on induced lift of fan area to wing area ratio and the combined effects of wing geometry, fan location, and fan distribution. In figure 23 induced lift of the present investigation is compared with previous conventional fan-in-wing data

(refs. 1, 2). Decreasing fan-to-wing area ratio of compared data gave increased induced lift as indicated in reference 6. Induced lift values for this model appear to be of the correct magnitude based on fan-area-to-wing-area ratio and the data of references 1 and 2.

Variation of pitching moment with airspeed is shown in figure 24 with BLC on and for three flap deflections. Pitching moment is nondimensionalized by the product of fan static thrust and diameter. The resulting pitching moment trend at zero flap deflection is characteristic of previous fan-in-wing investigations (refs. 2, 3, 7). The data show that with forward speed, increasing flap deflection reduces the change in pitching moment from that required for trim at hover.

Variable angle of attack- Power off longitudinal data shown in figure 11 agree well with established triangular wing data (ref. 8) for an aspect ratio of 2 with trailing-edge flaps undeflected. Figure 11 also shows data for 30° and 60° flap deflections. With power on, and BLC, the lift-curve slope (figs. 12(a) to 13(d)), in addition to varying with flap deflection, depends on the combined effects of exit vane deflection, forward velocity and its interaction with BLC jet velocity. As shown in figure 25, power-on lift-curve slopes were generally above the power-off value. It should be noted that the improvement in lift due to BLC, in figure 12(a), is hidden due to nondimensionalizing total lift with fan static thrust. The power-off portion of total lift does not increase with addition of BLC as does fan thrust. Hence with BLC on, the lift-to-static-thrust ratio is reduced.

A comparison of power-off data (fig. 11) with power-on data (figs. 12(a) to 13(d)) over the same angle-of-attack range showed that power on effects caused a point of maximum lift to occur which did not occur with power off. The effect of increasing forward speed, with power-on, was to increase the angle of attack for maximum lift. This angle of attack did not, however, reach 25° which was the highest power-off angle of attack tested. The power-on data of references 1 and 2 show that increasing forward speed had the opposite effect. This difference in trends might be explained by first noting where these investigations were similar. The point of maximum lift in each case was followed by a large destabilizing moment, indicating a loss in lift near the wing tip. Relating the forward speed effects and moment changes of the compared investigations to fan proximity to the wing leading edge might suggest the following explanation. The fans in references 1 and 2 were close to the wing leading edge and could delay lift loss by fan operation creating a large suction source, thus reducing leading-edge separation. The triangular wing of the present tests has the fan much farther from the wing leading edge, thereby eliminating such a strong suction effect. Increasing forward speed would then only create a Reynolds number effect that would increase the angle of attack for maximum lift.

Static margin is shown in figure 26 to be nearly constant except at a velocity ratio of 0.3 where a destabilizing effect occurred. This destabilizing tendency was greater with BLC applied. Exit vane deflection at each velocity ratio was that required to cause thrust equal to drag at zero angle of attack. Data included with essentially zero thrust vectoring (exit vanes

off) show only small changes in stability and thereby indicate limited interference of fan exhaust with wing flow. The option to choose from a wide range of fan thrust vector angles can be useful when planning aircraft descent angles.

Use of trailing-edge flaps was generally beneficial to the total lift even though they reduced the induced portion of total lift. The data for 60° flap deflection at low forward speeds (figs. 12(a) and 13) show a definite improvement both in the lift with drag trimmed (α = 0°) and in maximum lift.

CONCLUDING REMARKS

Results of an investigation of a supersonic aircraft configuration with a thin fan mounted in a triangular wing indicate fan thickness can be reduced without loss of static thrust by inclusion of a blowing BLC inlet.

Effects of fan operation on model performance, stability and control indicate no large adverse deviations from general delta wing characteristics. Therefore, V/STOL capability provided by lift fans for this supersonic configuration appears feasible.

Ames Research Center
National Aeronautics and Space Administration
Moffett Field, Calif., 94035, Aug. 30, 1970

REFERENCES

1. Hickey, David H.; and Hall, Leo P.: Aerodynamic Characteristics of a Large-Scale Model With Two High Disk-Loading Fans Mounted in the Wing. NASA TN D-1650, 1963.

2. Kirk, Jerry V.; Hickey, David H.; and Hall, Leo P.: Aerodynamic Characteristics of a Full-Scale Fan-In-Wing Model Including Results in Ground Effect With Nose-Fan Pitch Control. NASA TN D-2368, 1964.

3. Cook, Woodrow L.; and Hickey, David H.: Comparison of Wind-Tunnel and Flight-Test Aerodynamic Data in the Transition-Flight Speed Range for Five V/STOL Aircraft. Conference on V/STOL and STOL Aircraft. NASA SP-116, 1966, pp. 447-467.

4. Przedpelski, Zygmunt J.: Lift Fan Technology Studies. NASA CR-761, 1967.

5. Aoyagi, Kiyoshi; Hickey, David H.; and deSavigny, Richard A.: Aerodynamic Characteristics of a Large-Scale Model With a High Disk-Loading Lifting Fan Mounted in the Fuselage. NASA TN D-775, 1961.

6. Goldsmith, Robert H.; and Hickey, David H.: Characteristics of Lifting-Fan V/STOL Aircraft. Astronautics and Aerospace Engineering, vol. 1, no. 9, Oct. 1963, pp. 70-77.

7. Kirk, Jerry V.; Hodder, Brent K.; and Hall, Leo P.: Large-Scale Wind-Tunnel Investigation of a V/STOL Transport Model With Wing-Mounted Lift-Fans and Fuselage-Mounted Lift-Cruise Engines for Propulsion. NASA TN D-4233, 1967.

8. Graham, David: The Low-Speed Lift and Drag Characteristics of a Series of Airplane Models Having Triangular or Modified Triangular Wings. NACA RM A53D14, 1953.

TABLE 1.- COORDINATES OF WING AIRFOIL SECTION (NACA 16-005 MODIFIED)

PERPENDICULAR TO THE WING CHORD PLANE

	Upper	Lower
x/c	y/c	y/c
0	0	0
1.25	.563	.513
2.50	.801	.703
5.00	1.136	.944
7.50	1.405	1.123
10.00	1.624	1.258
15.00	1.986	1.461
20.00	2.276	1.610
30.00	2.709	1.809
40.00	2.970	1.907
50.00	3.083	1.917
60.00	3.030	1.830
70.00	2.758	1.633
80.00	2.199	1.299
90.00	1.307	.781
95.00	.731	.449
100.00	.050	.050

TABLE 2.- LIST AND DESCRIPTION OF BASIC DATA FIGURES

Figure	α, deg	β_V, deg	V, knots	δ_F, deg	Remarks
Lift-fan performance					
7	0	0	20, 30, 40 60, 80	30	Relationship of velocity ratio to tip-speed ratio
8	0	0	0	30	Static thrust calibration of all fan configurations tested
9	0	0	20, 30, 40 60, 80	30	Fan thrust variation with forward speed, BLC on BLC off
Longitudinal data at zero angle of attack; C_L, C_D, C_m, versus μ					
10(a)	0	0, 10, 20 30, 40, 50	20, 30, 40 60, 80	0	With BLC
10(b)					
10(c)					
10(d)				30	With BLC
10(e)					
10(f)					Without BLC
10(g)					
10(h)				60	With BLC
10(i)					
Longitudinal data at variable angle of attack C_L versus C_D, α, C_m					
11	-4 to 24	90	80	0, 30, 60	Lift fan not operating, fan inlets sealed
12(a)		12 (trim)	30	0, 30, 60	With and without BLC; L/Ts versus D/T_S, α, $M/T_S D_F$
12(b)		off	30	30	
13(a)		18 (trim)	40	0, 30, 60	With and without BLC
13(b)		off	40	30	
13(c)		36 (trim) and off	60	0, 30, 60	
13(d)		50°	80, 100	0, 30, 60	

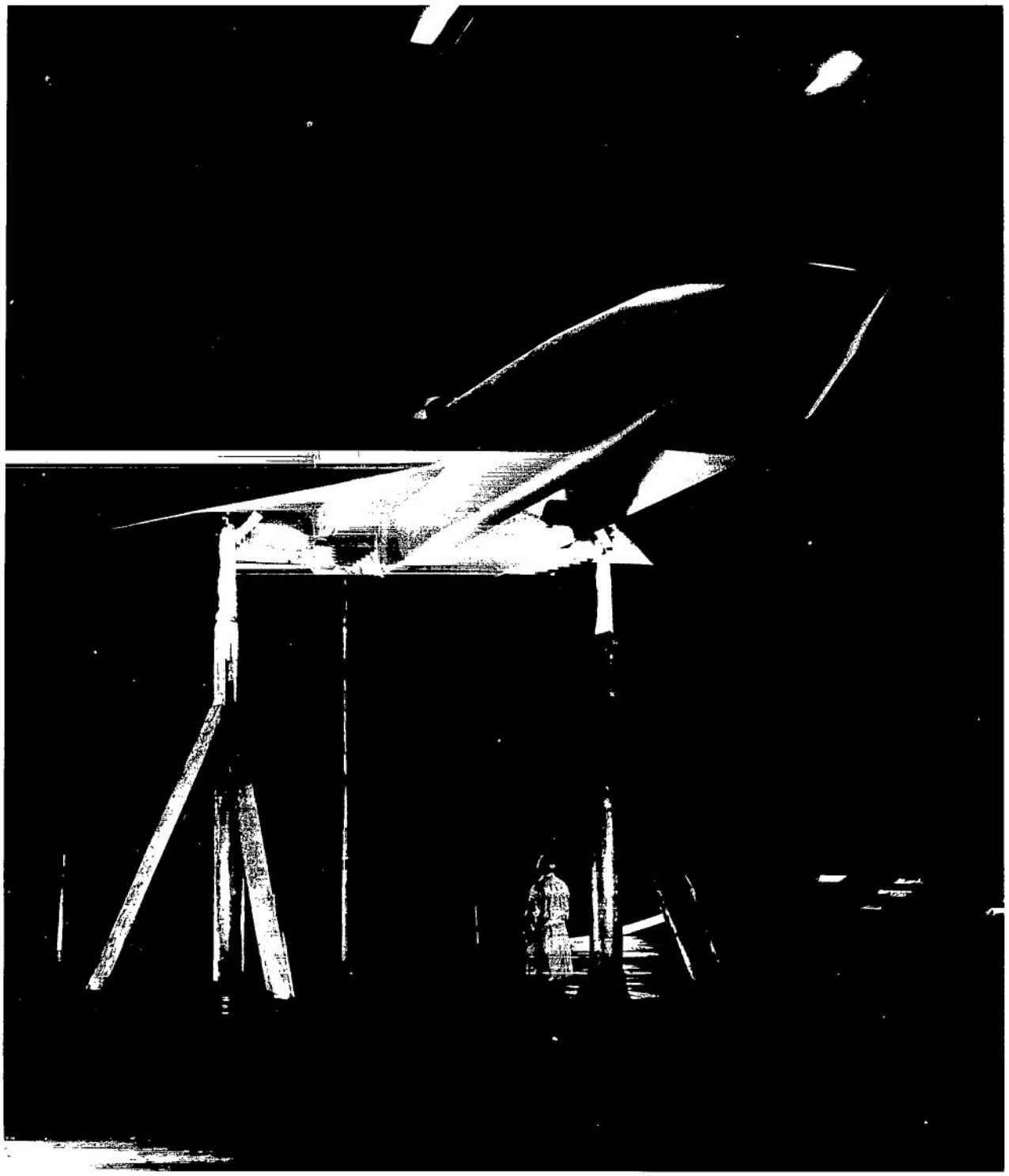

(a) 3/4 front view.

A-37808

Figure 1.- Photograph of model mounted in Ames 40- by 80-Foot Wind Tunnel.

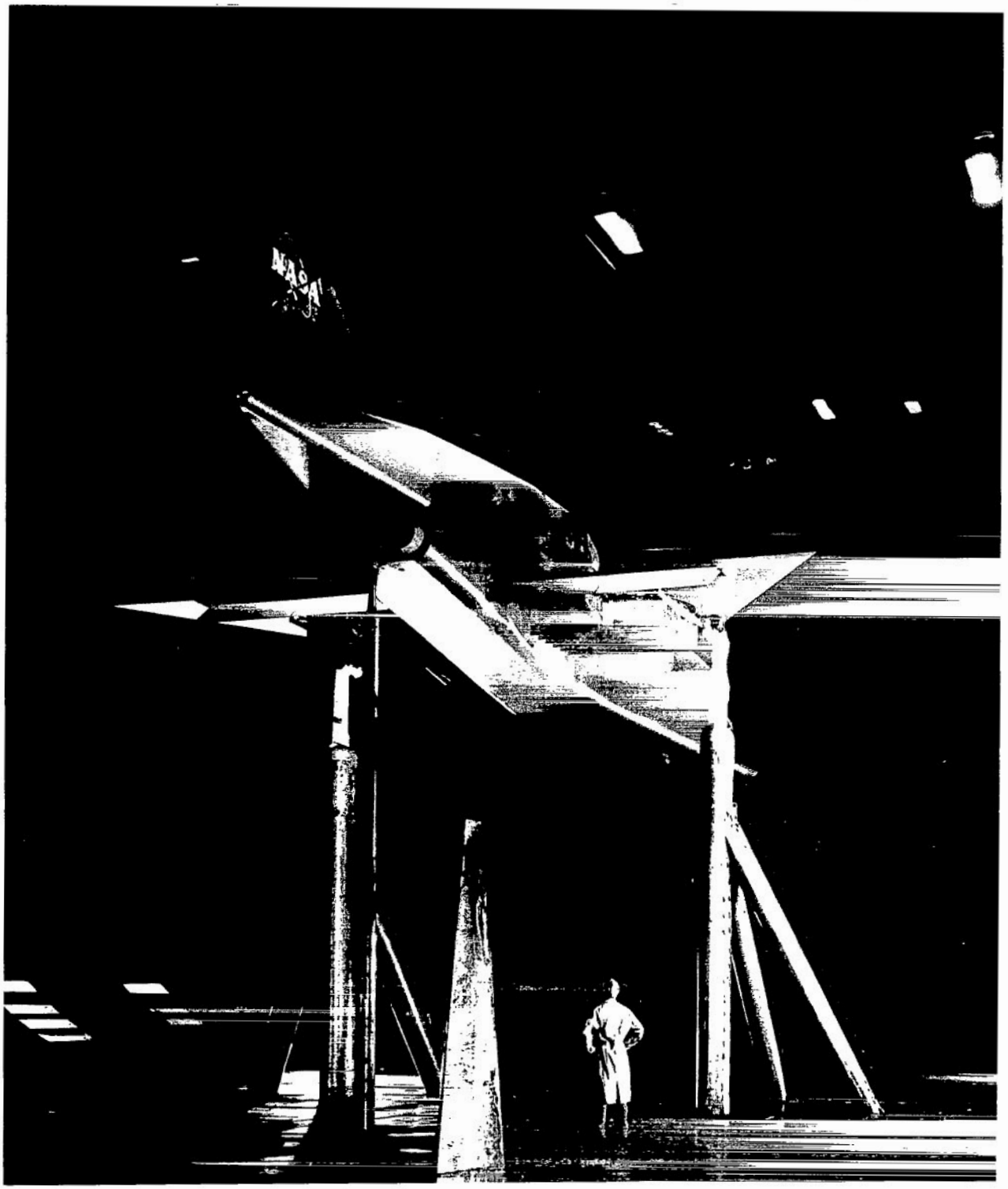

A-37809

(b) 3/4 rear view.

Figure 1.- Continued.

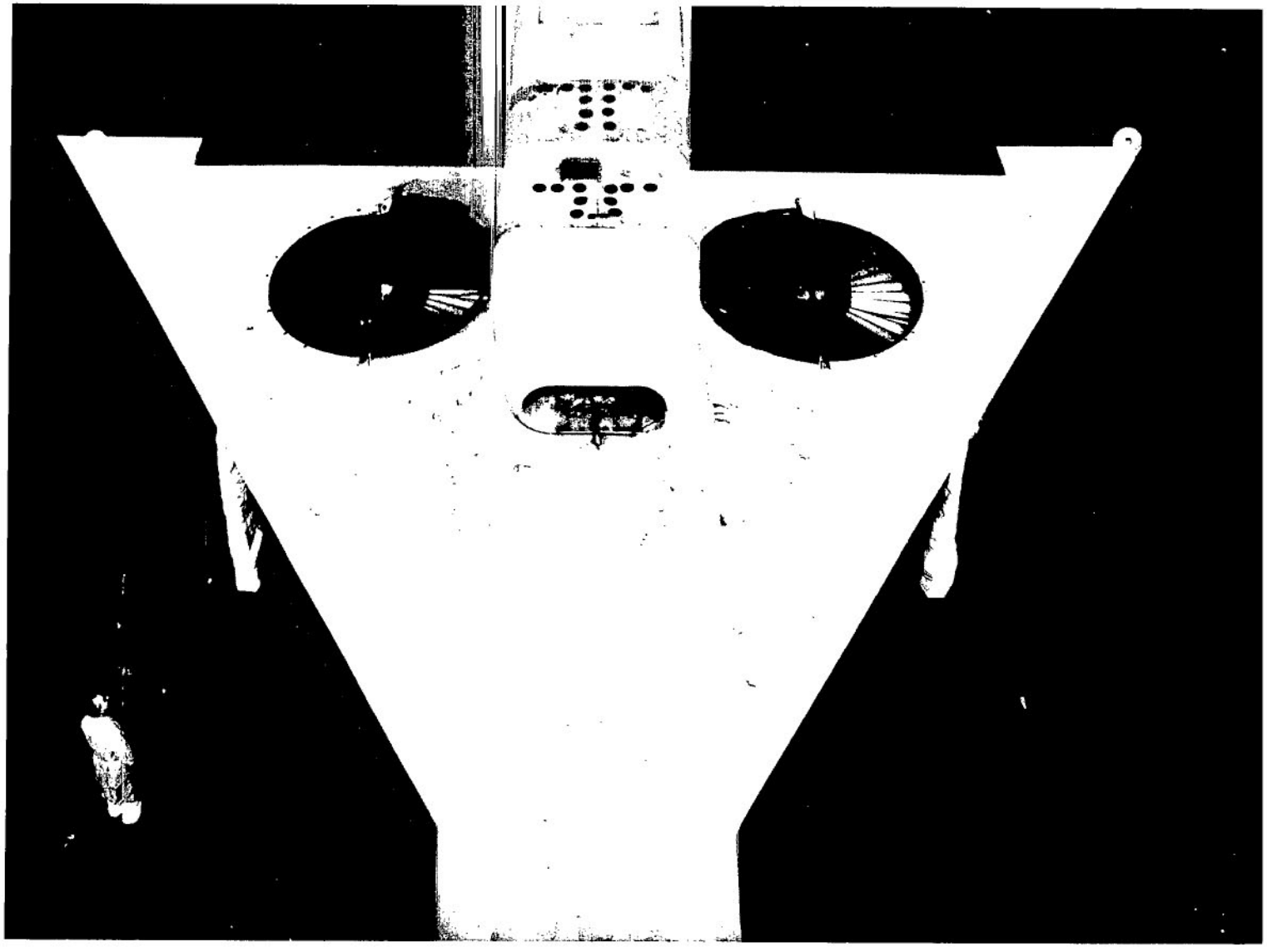

A-38863

(c) Top view.

Figure 1.- Concluded.

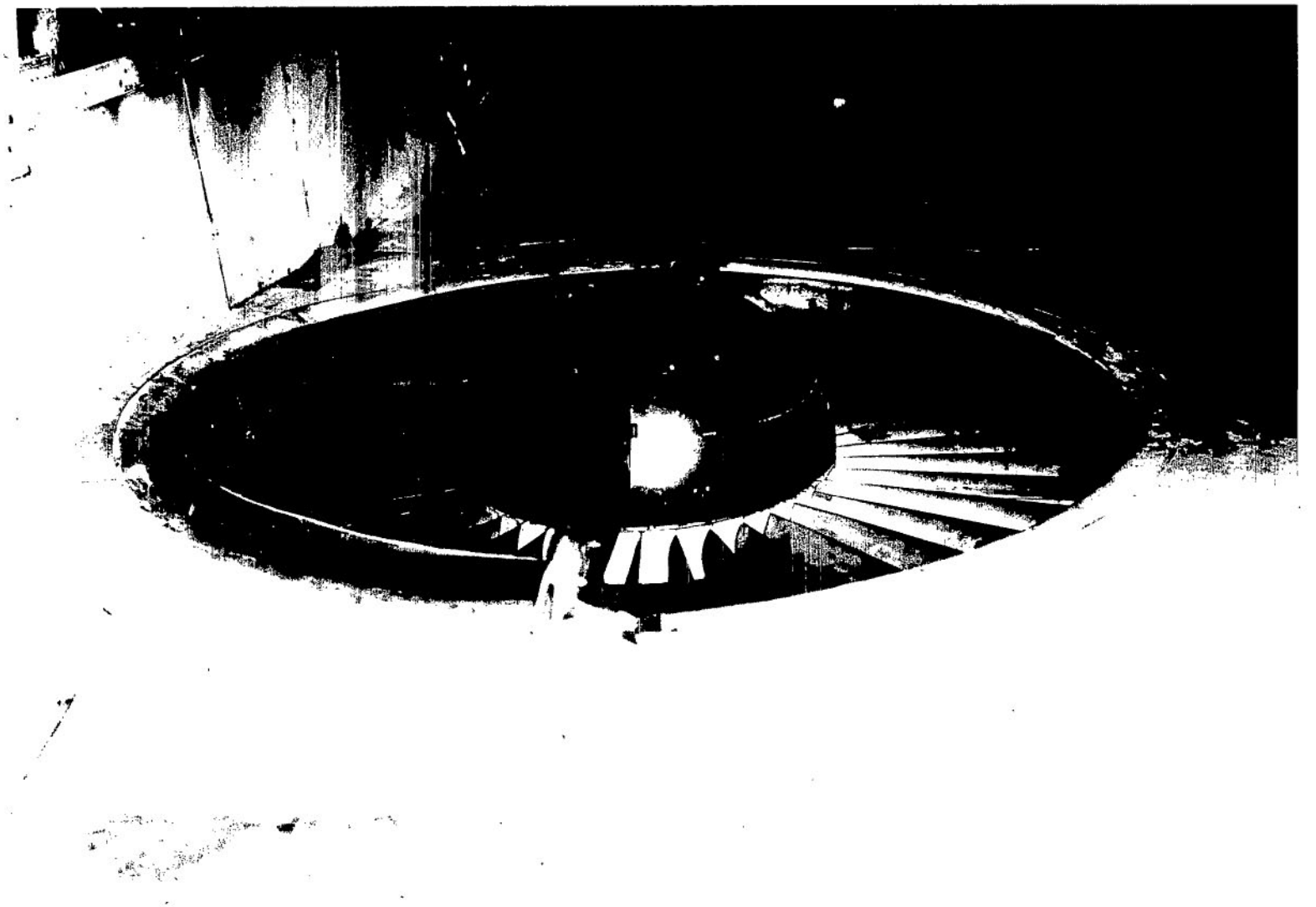

A-38944

Figure 2.- Photograph of right lift-fan showing boundary-layer-control inlet.

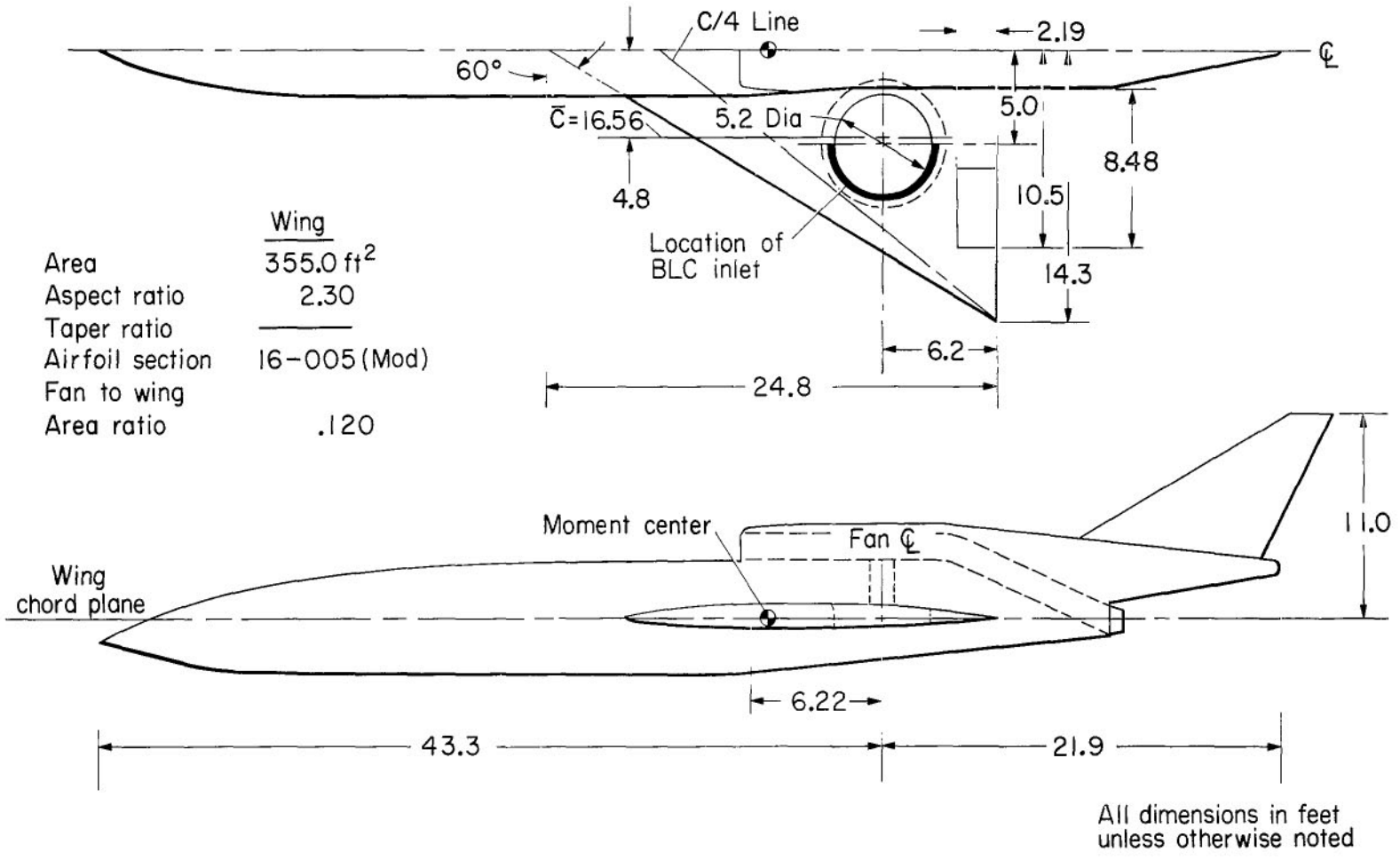

Figure 3.- General arrangement of triangular wing, lift-fan model.

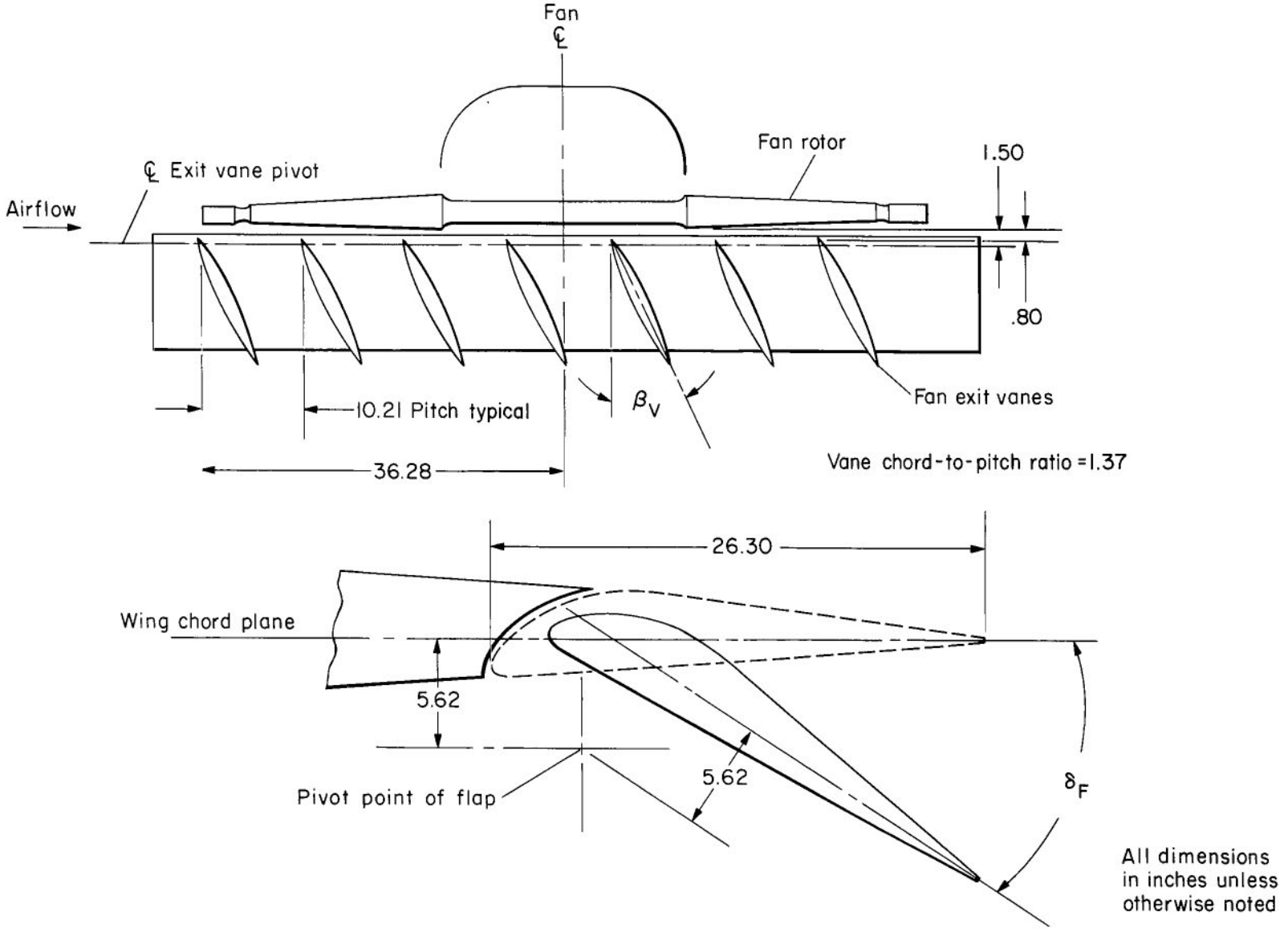

Figure 4.- Details of trailing-edge flaps and fan exit vanes.

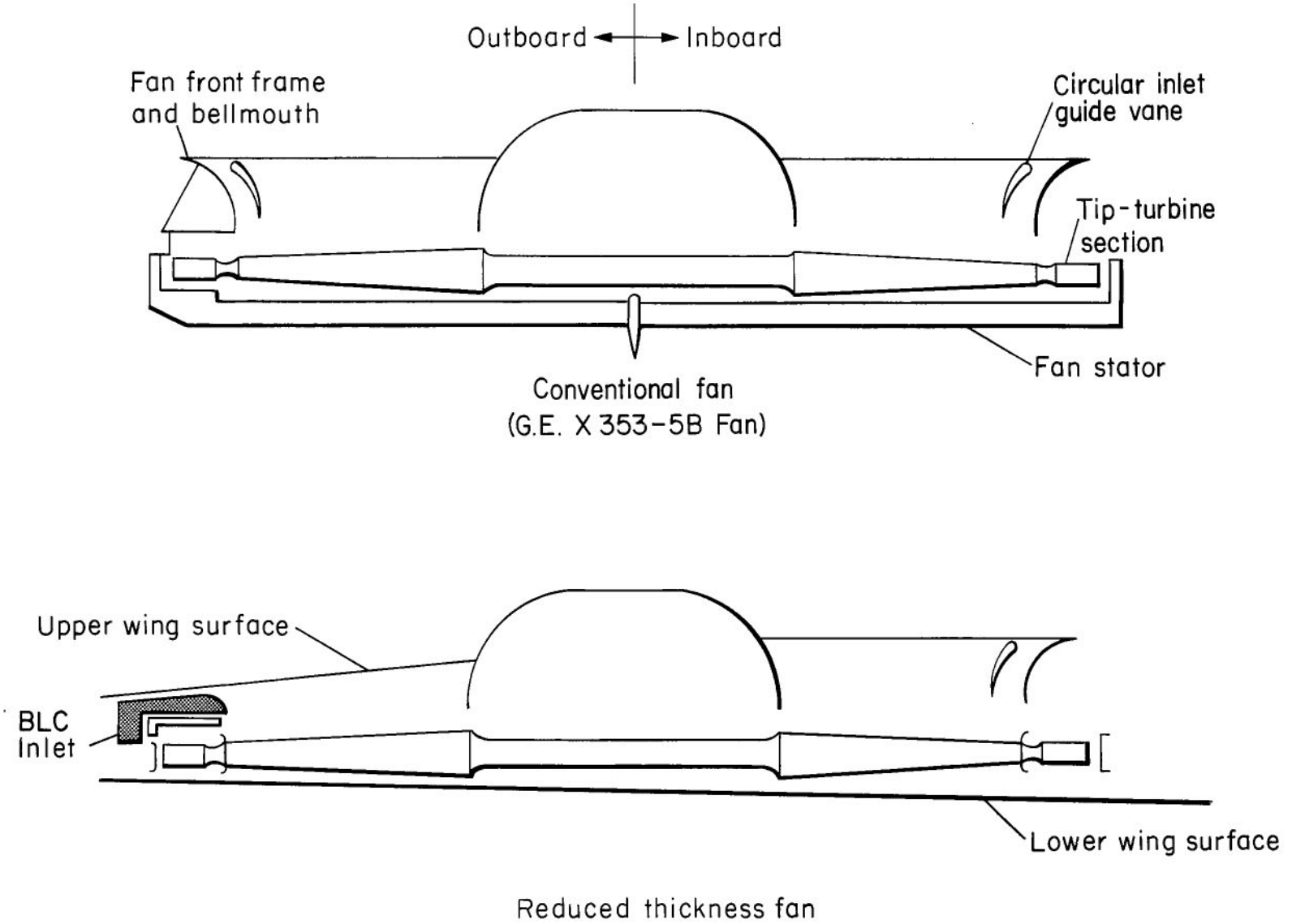

Figure 5.- Generalized lift-fan modification.

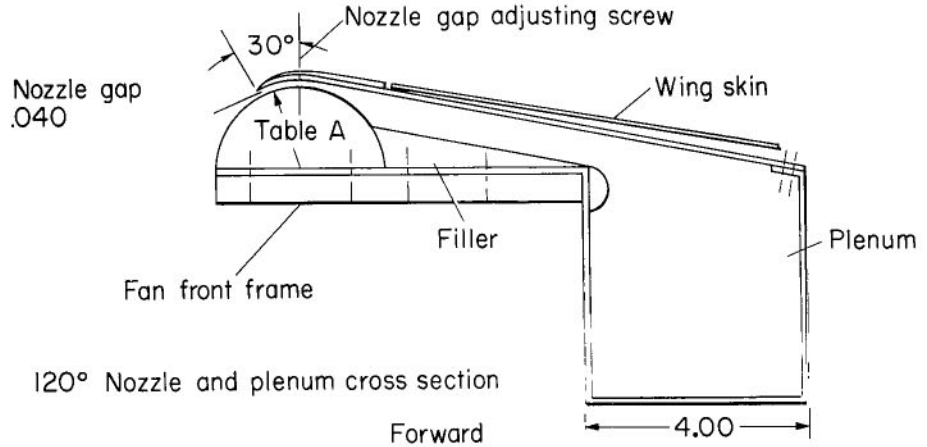

120° Nozzle and plenum cross section

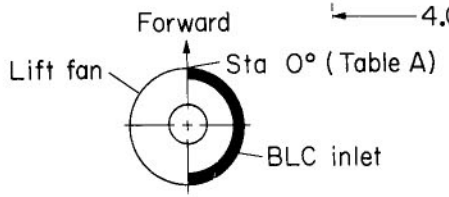

Table A

Sta	Radius
0°	3.45
15°	2.75
30°	2.25
45°	1.85
60°	1.56
75°	1.41
90°	1.46
105°	1.57
120°	1.64
135°	1.66
150°	1.56
165°	1.46
180°	1.50

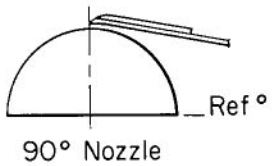

90° Nozzle

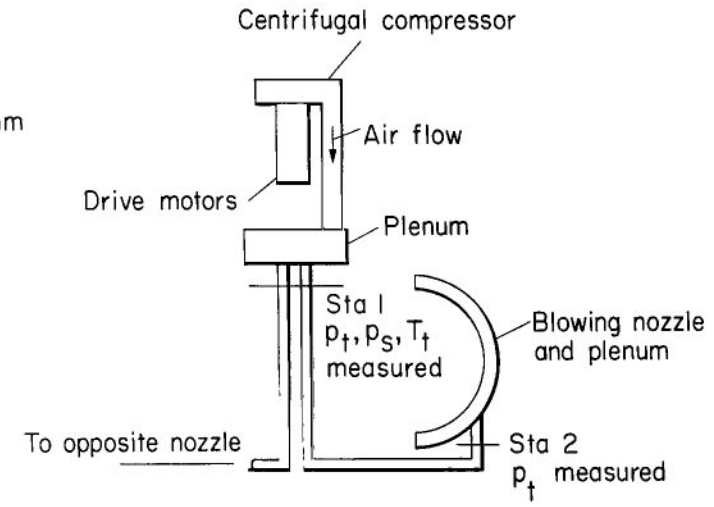

Blowing BLC system schematic

All dimensions in inches
unless otherwise noted

Figure 6.- Details of BLC nozzle.

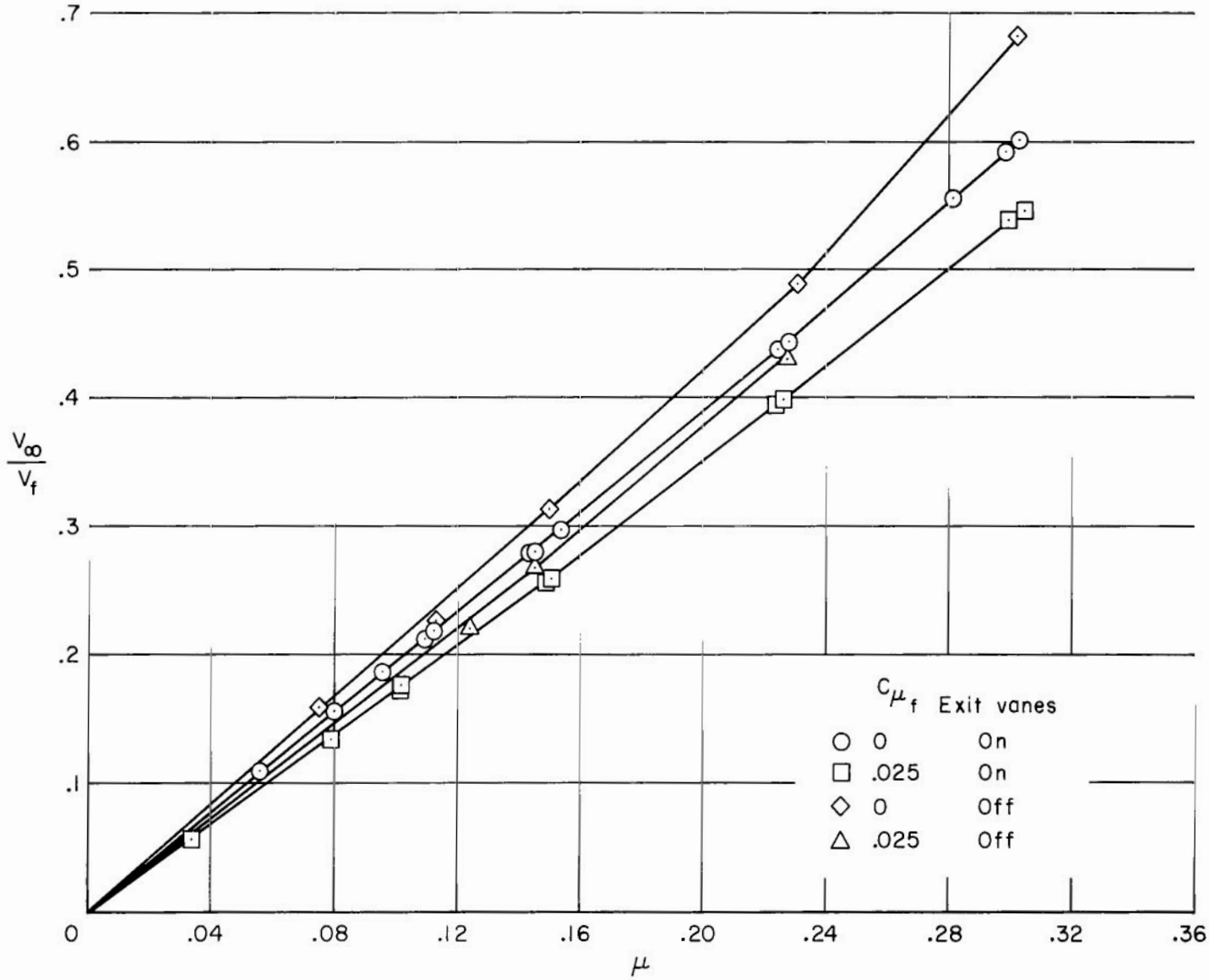

Figure 7.- Variation of average velocity ratio with tip speed ratio; $\beta_v = 0°$, $\alpha = 0°$, 1700 rpm.

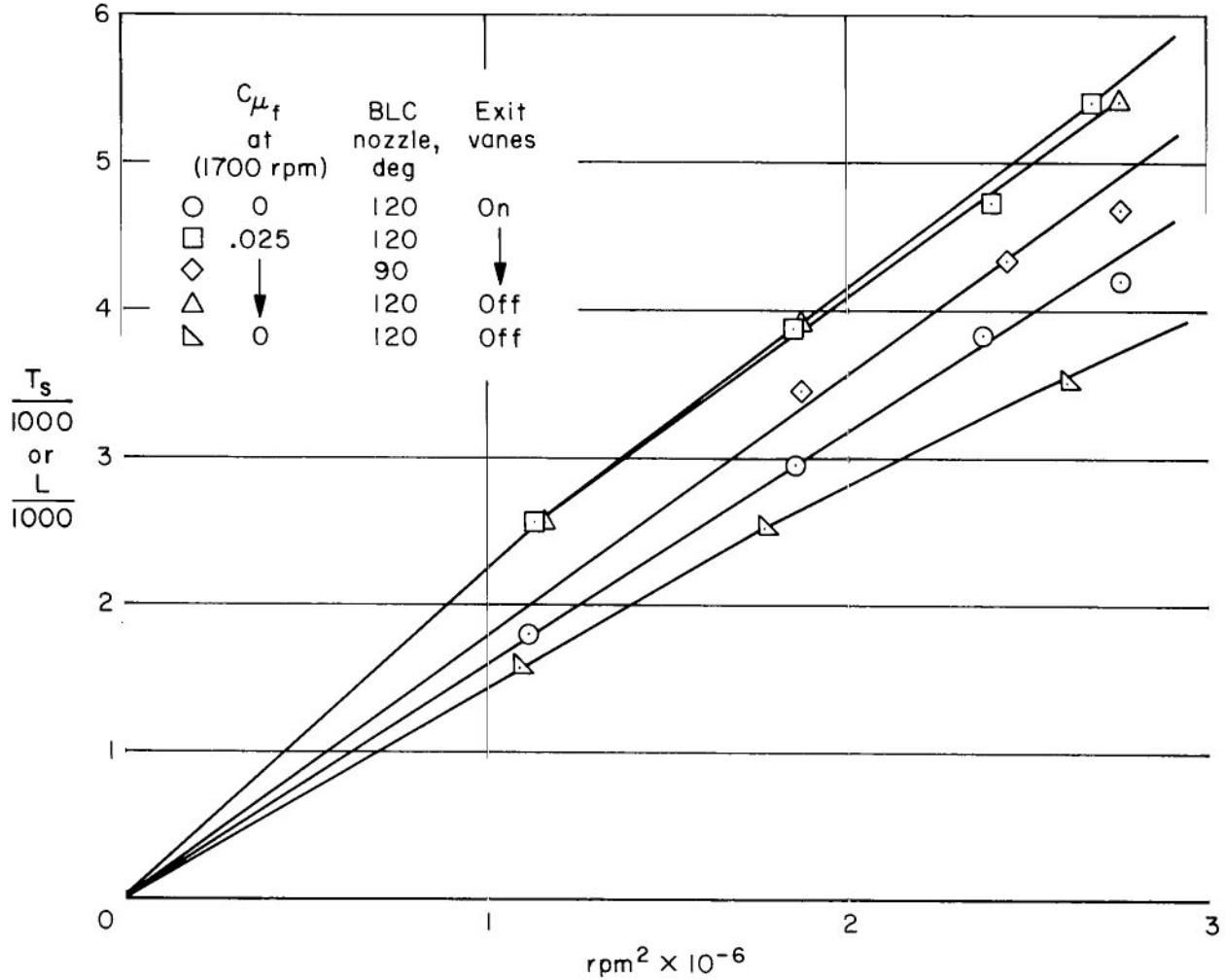

Figure 8.- Fan static thrust; $V_\infty = 0$, $\beta_V = 0°$, both fans, constant BLC momentum when in use.

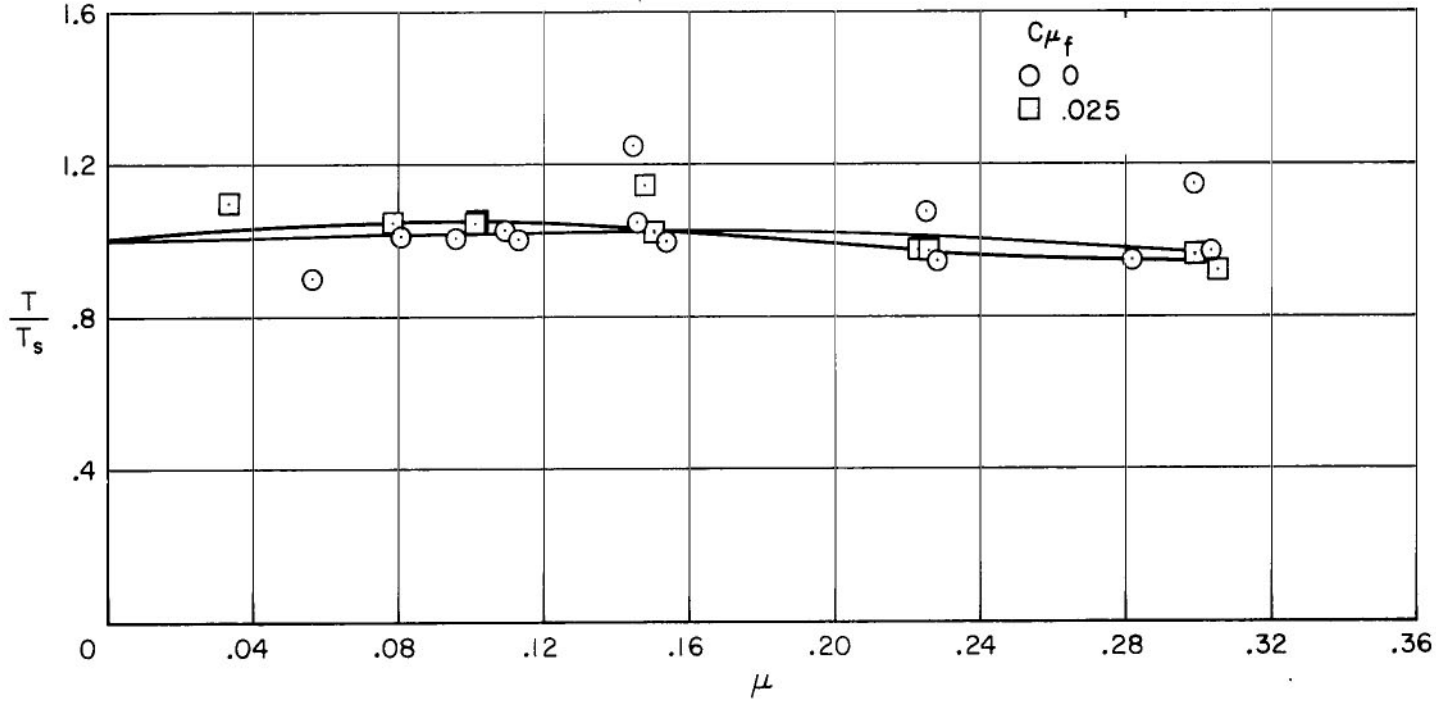

Figure 9.- Effect of forward speed (tip-speed ratio) on fan thrust; $\alpha = 0°, 1700$ rpm, $\beta_v = 0°$.

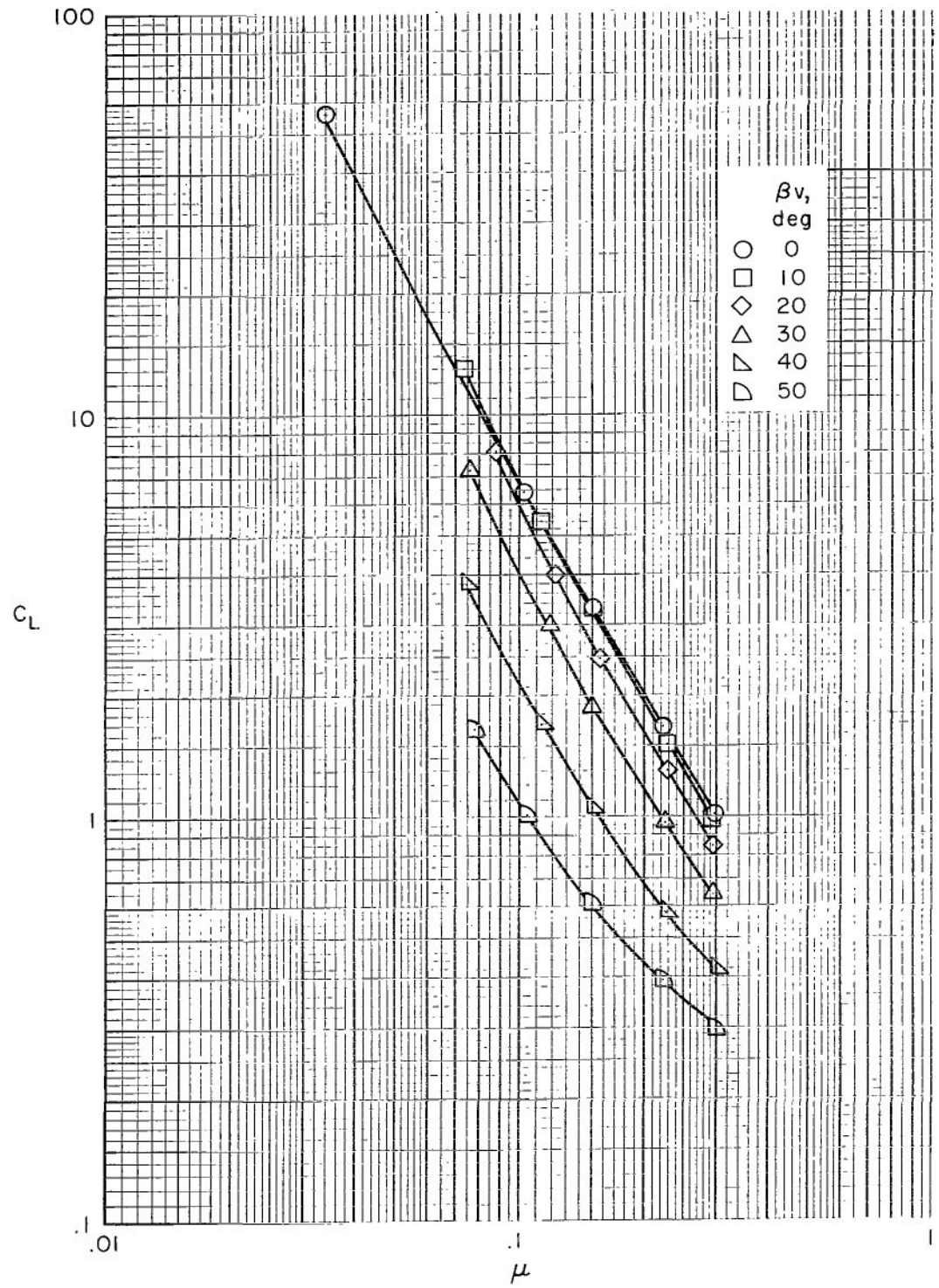

(a) C_L vs μ, $\delta_F = 0°$, $C_{\mu_f} = 0.025$

Figure 10.- Variation of longitudinal characteristics with tip-speed ratio; 1700 rpm, $\alpha = 0°$.

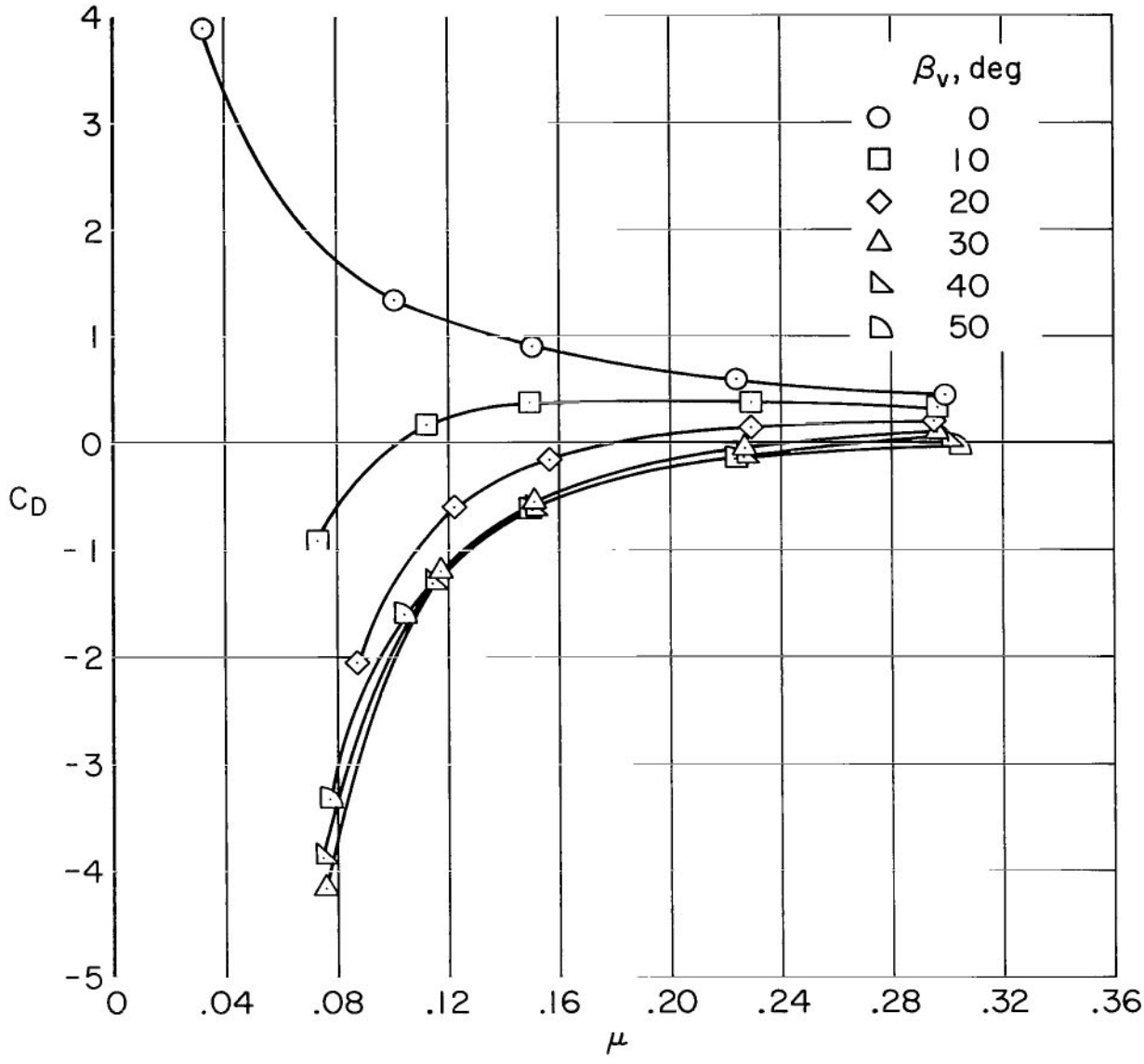

(b) C_D vs μ, $\delta_F = 0°$, $C_{\mu_f} = 0.025$

Figure 10.- Continued.

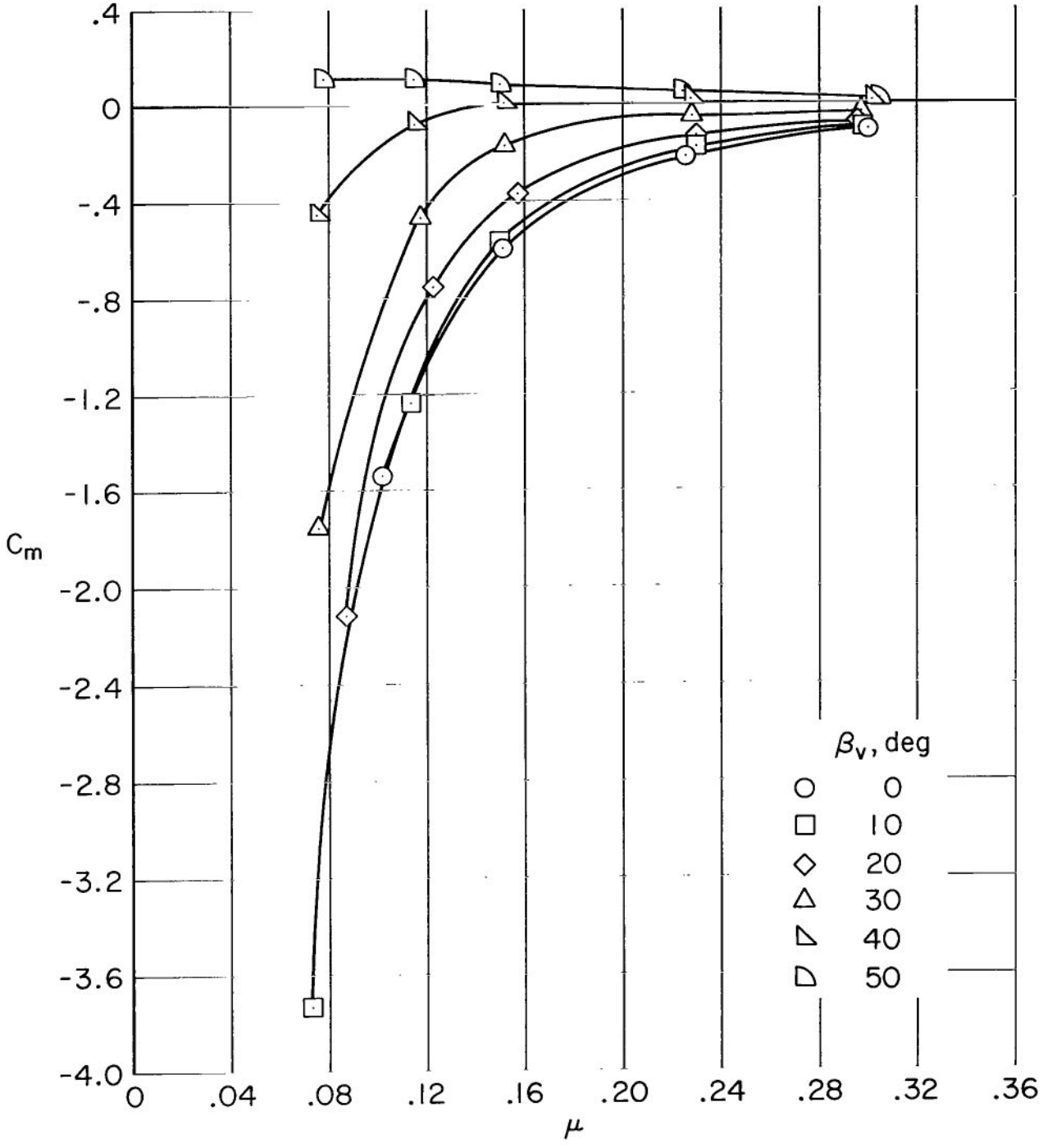

(c) C_m vs μ, $\delta_F = 0°$, $C_{\mu_f} = 0.025$

Figure 10.- Continued.

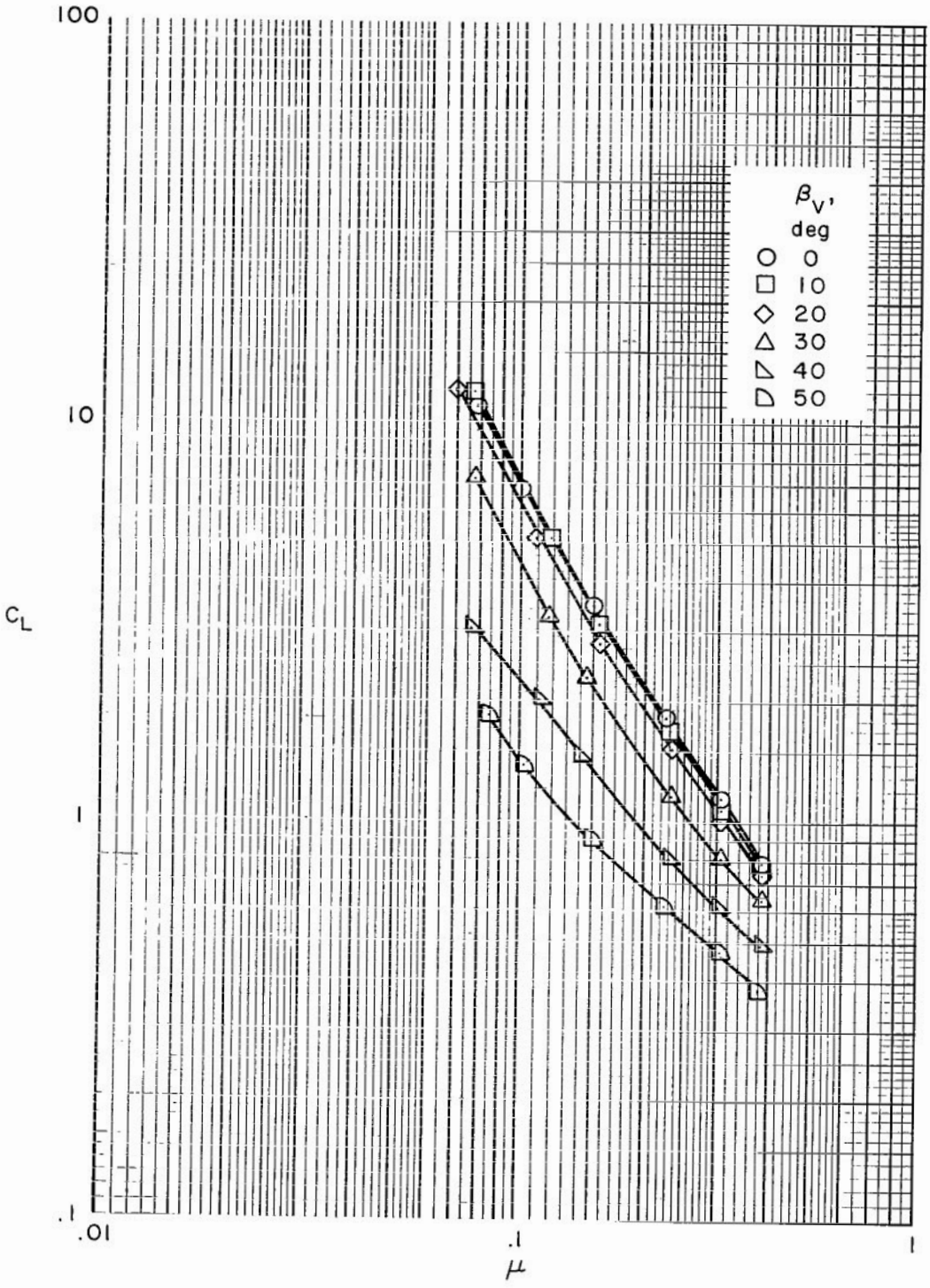

(d) C_L vs μ, $\delta_F = 30°$, $C_{\mu_f} = 0.025$

Figure 10.- Continued.

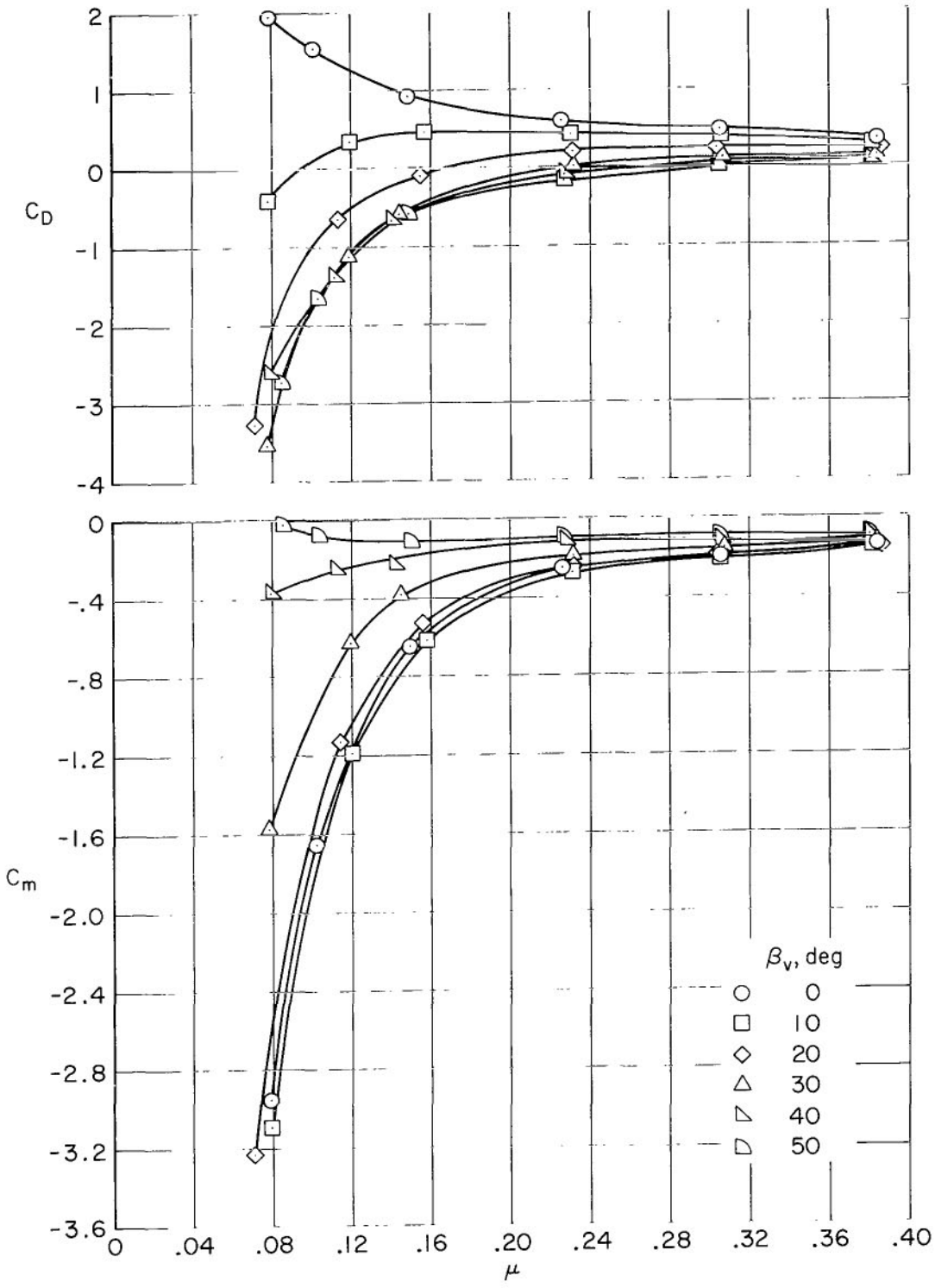

(e) C_D, C_m vs μ, $\delta_F = 30°$, $C_{\mu_f} = 0.025$

Figure 10.- Continued.

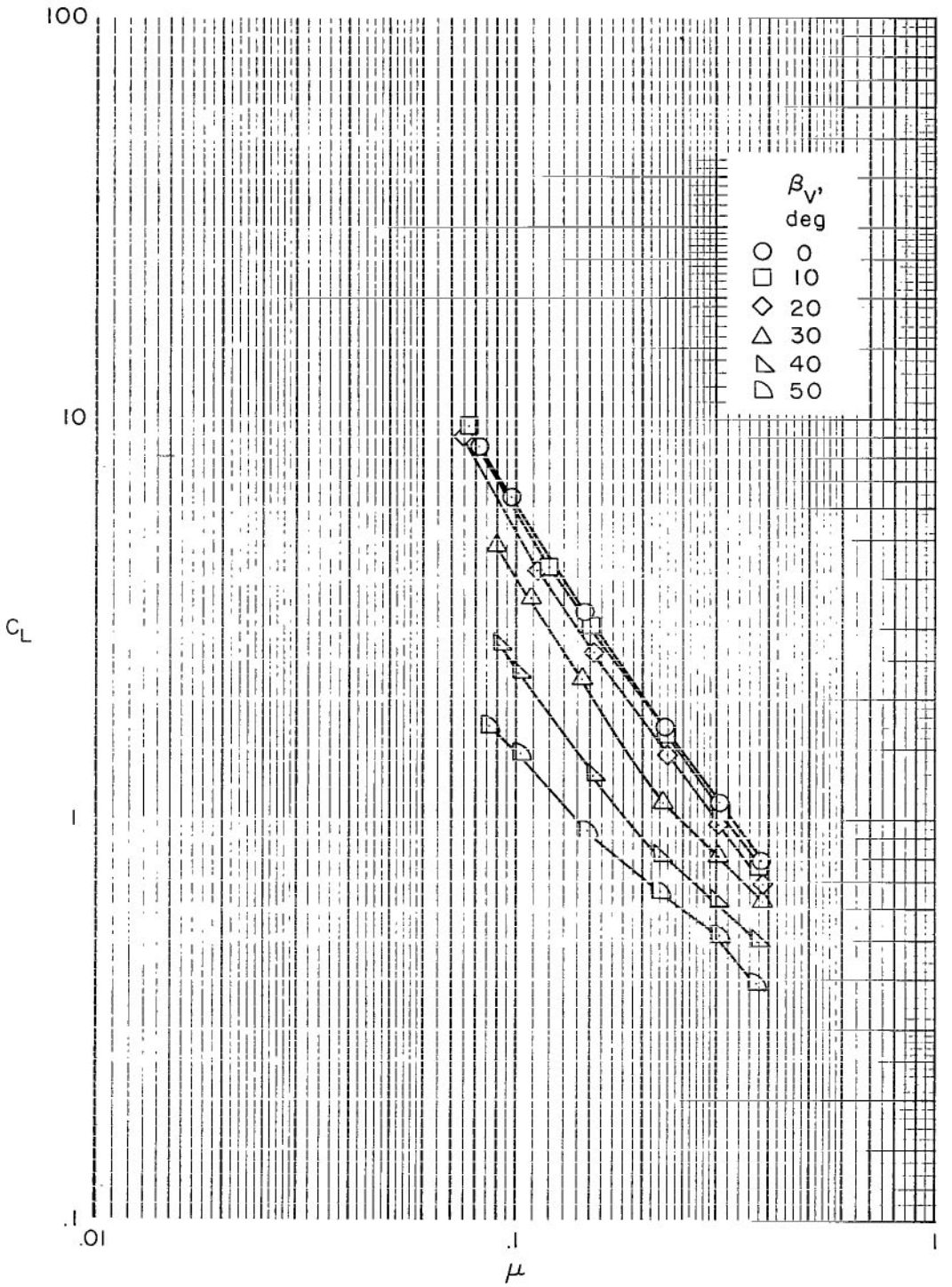

(f) C_L vs μ, $\delta_F = 30°$, $C_{\mu_f} = 0$

Figure 10.- Continued.

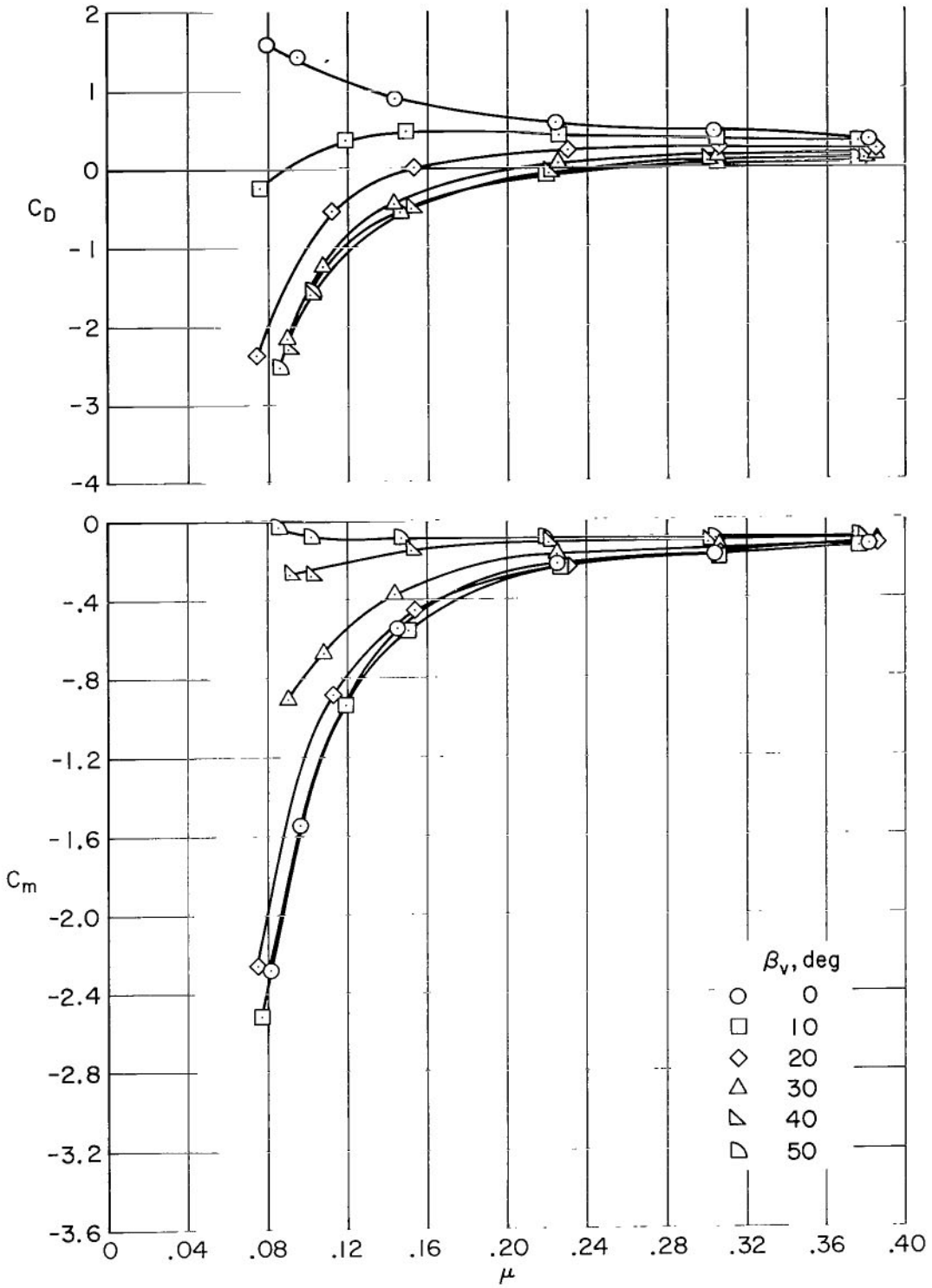

(g) C_D, C_m vs μ, $\delta_F = 30°$, $C_{\mu_f} = 0$

Figure 10.- Continued.

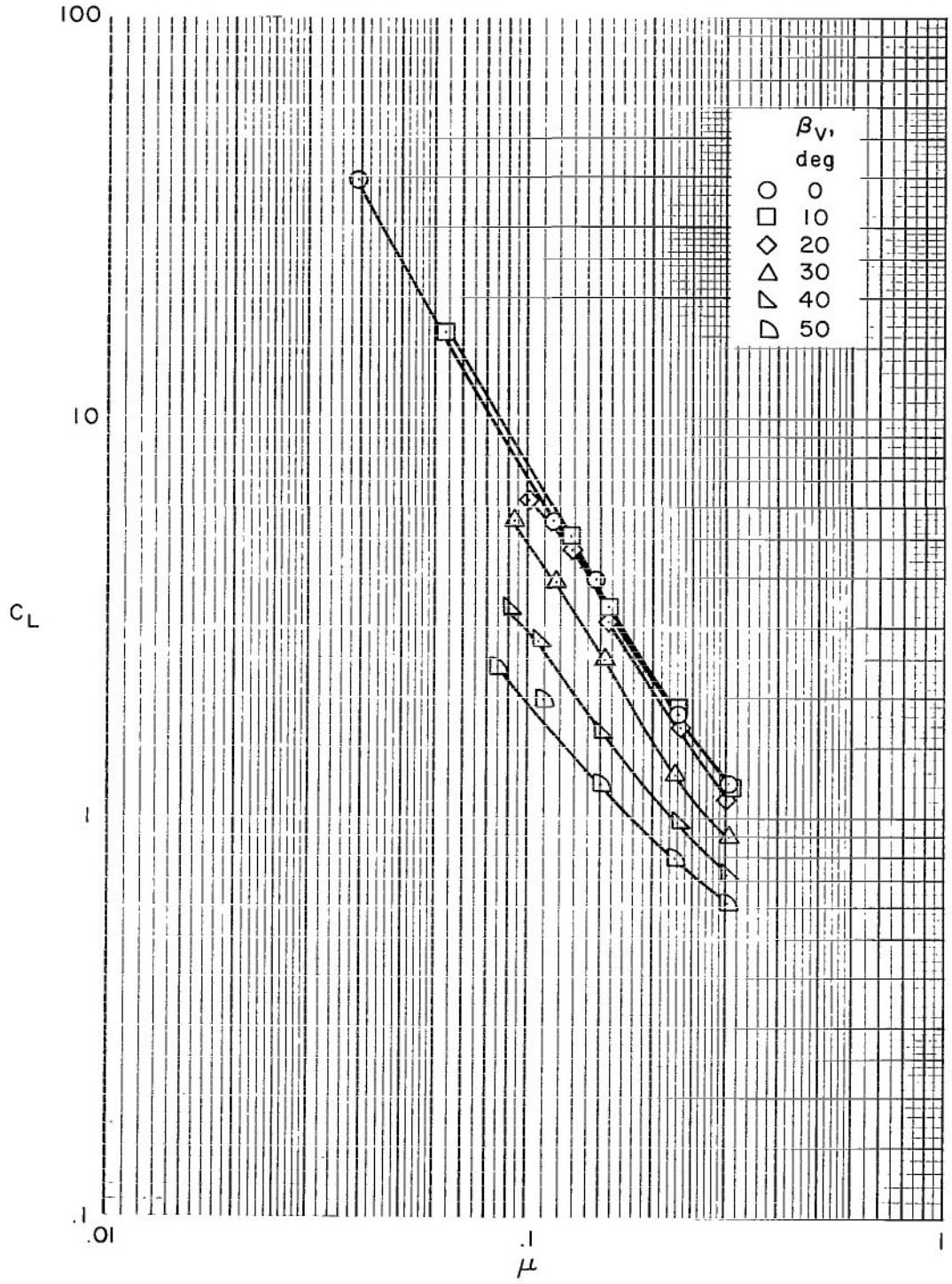

(h) C_L vs μ, $\delta_F = 60°$, $C_{\mu_f} = 0.025$

Figure 10.- Continued.

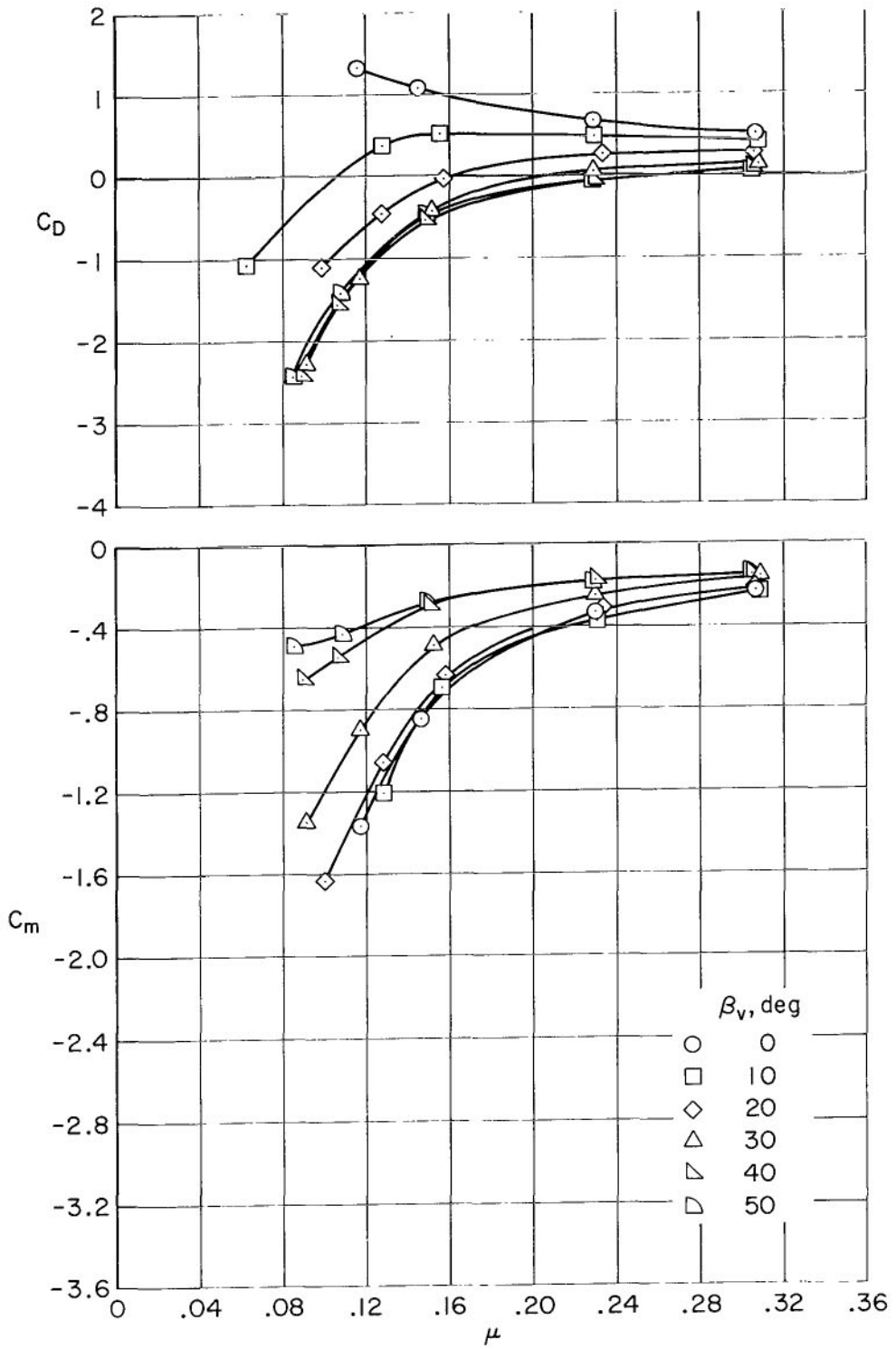

(i) C_D, C_m vs μ, $\delta_F = 60°$, $C_{\mu_f} = 0.025$

Figure 10.- Concluded.

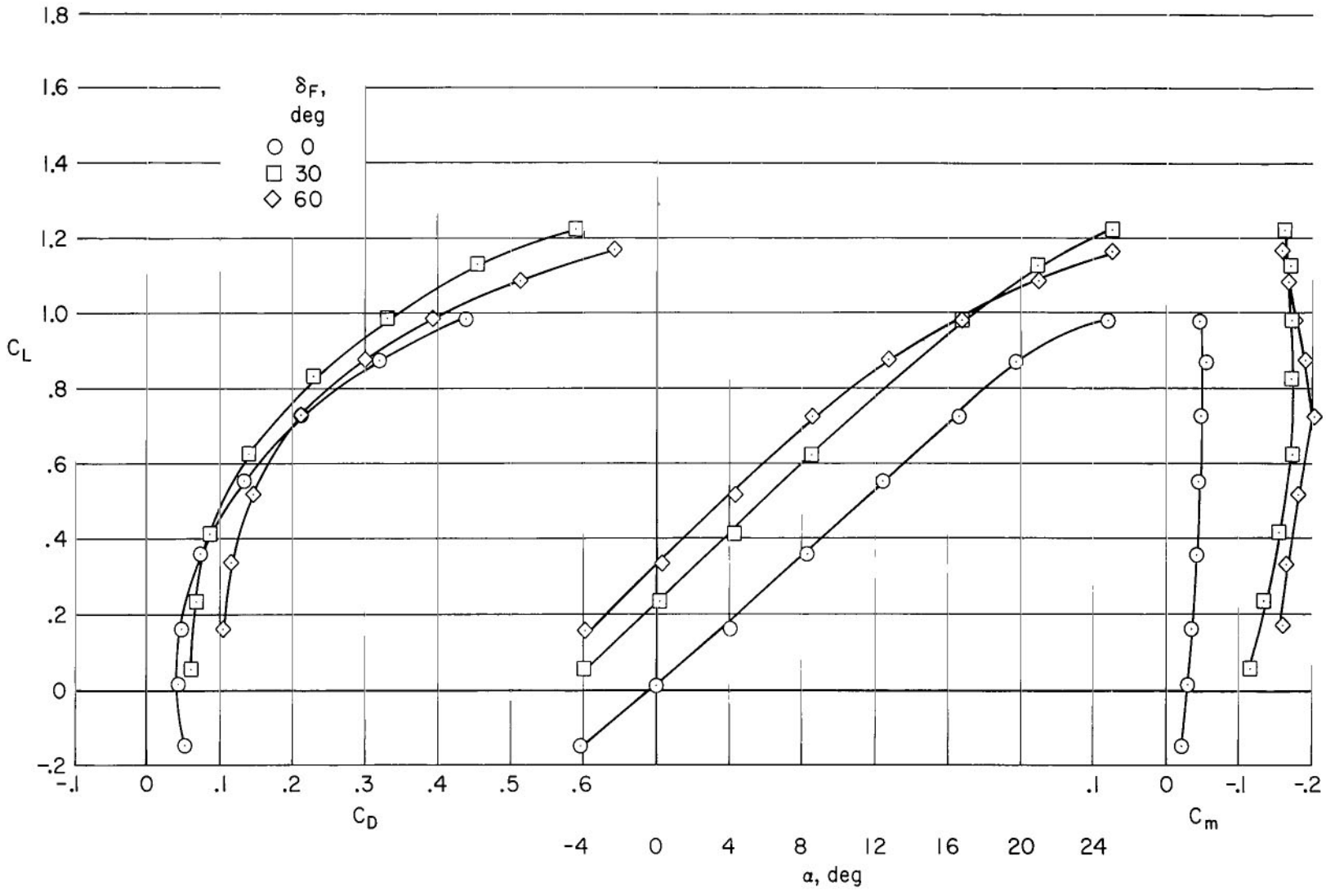

Figure 11.- Longitudinal characteristics with power off; fan inlets sealed, β_V = 90°, and V_∞ = 80 knots.

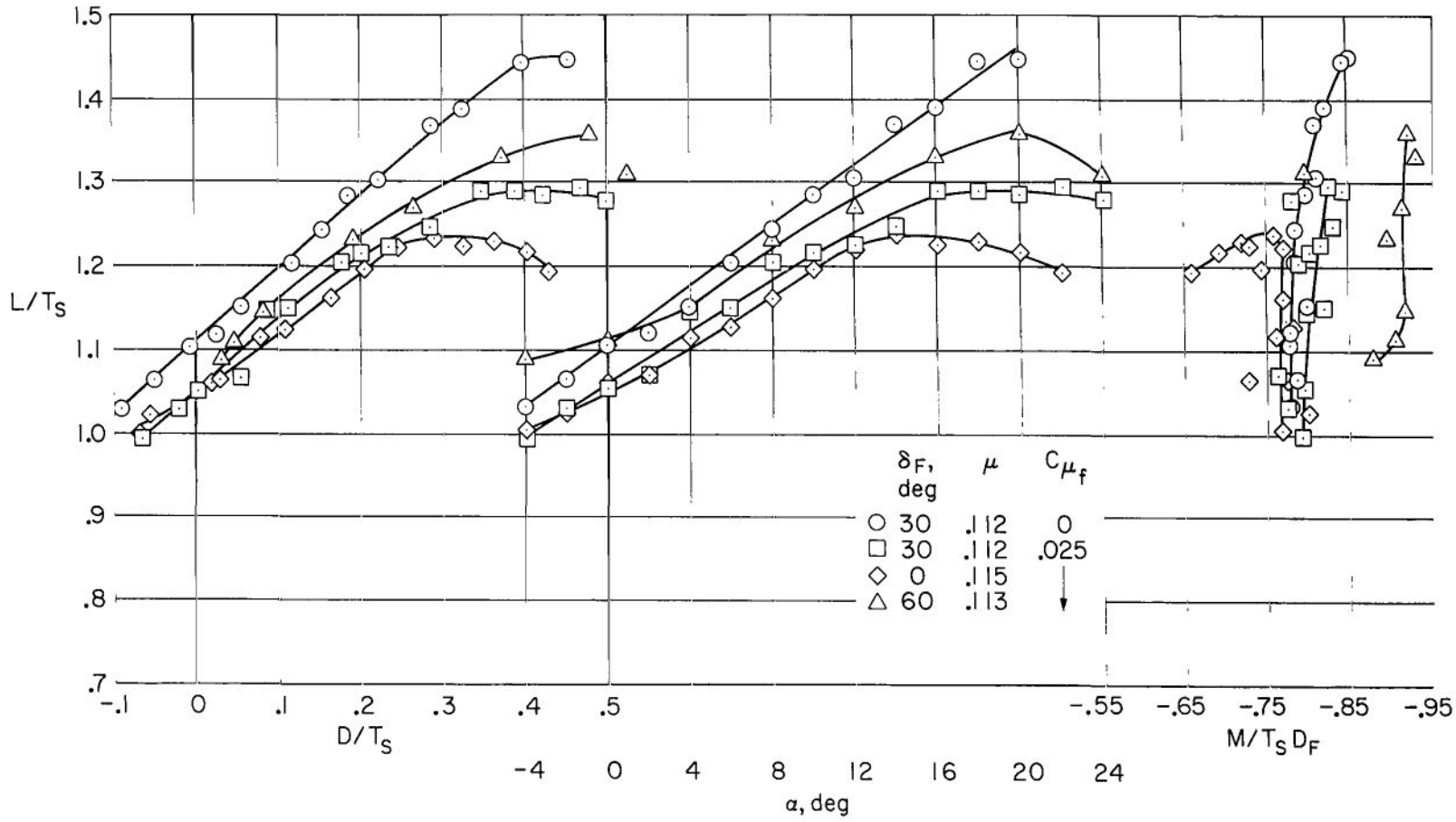

(a) Exit vanes on.

Figure 12.- Longitudinal characteristics with power on; 1700 rpm, β_V = 12°, and V_∞ = 30 knots.

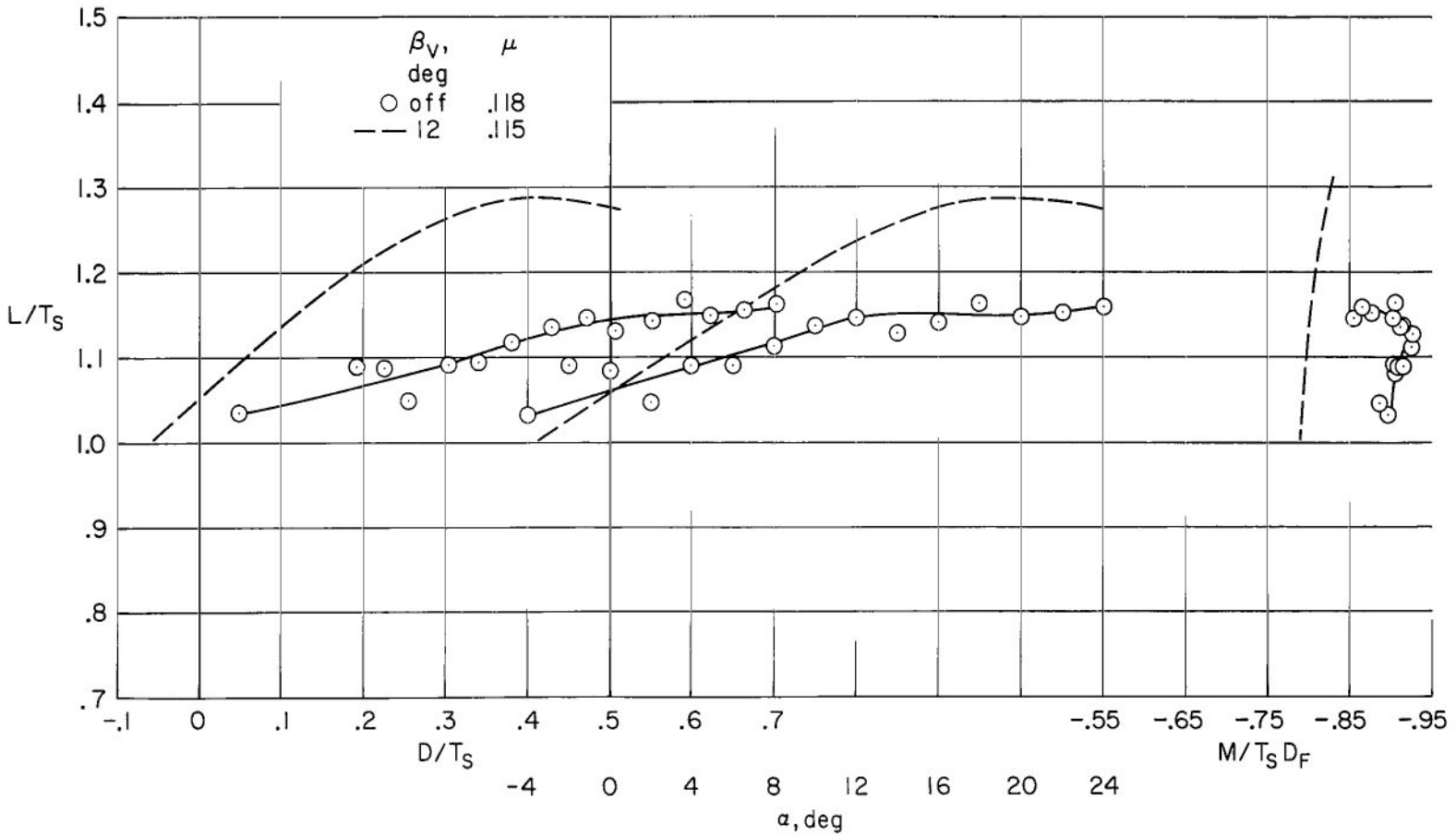

(b) Exit vanes off, $\delta_F = 30°$, $C_{\mu_f} = 0.025$.

Figure 12.- Concluded.

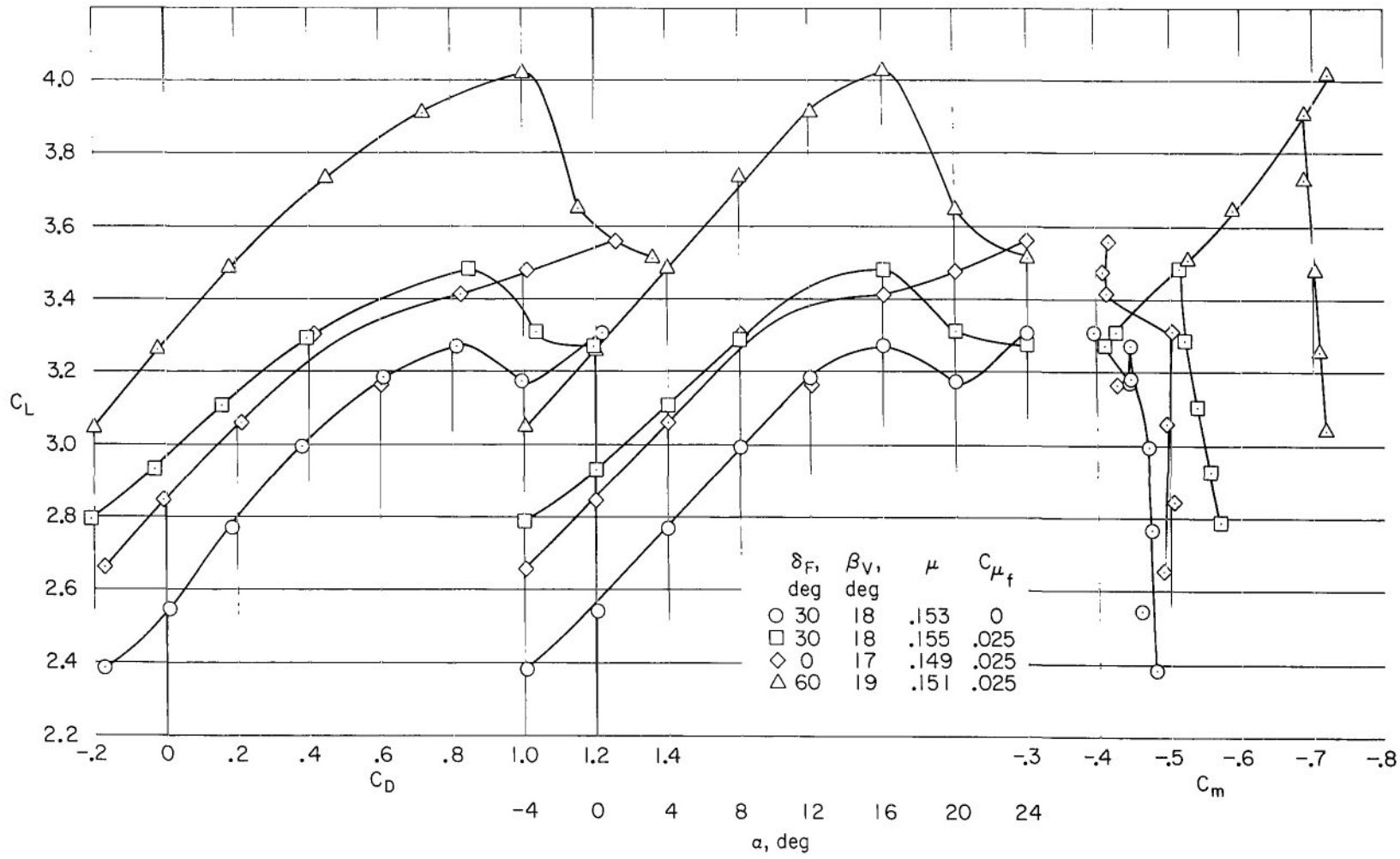

(a) Exit vanes on, V_∞ = 40 knots.

Figure 13.- Longitudinal characteristics with power on; 1700 rpm.

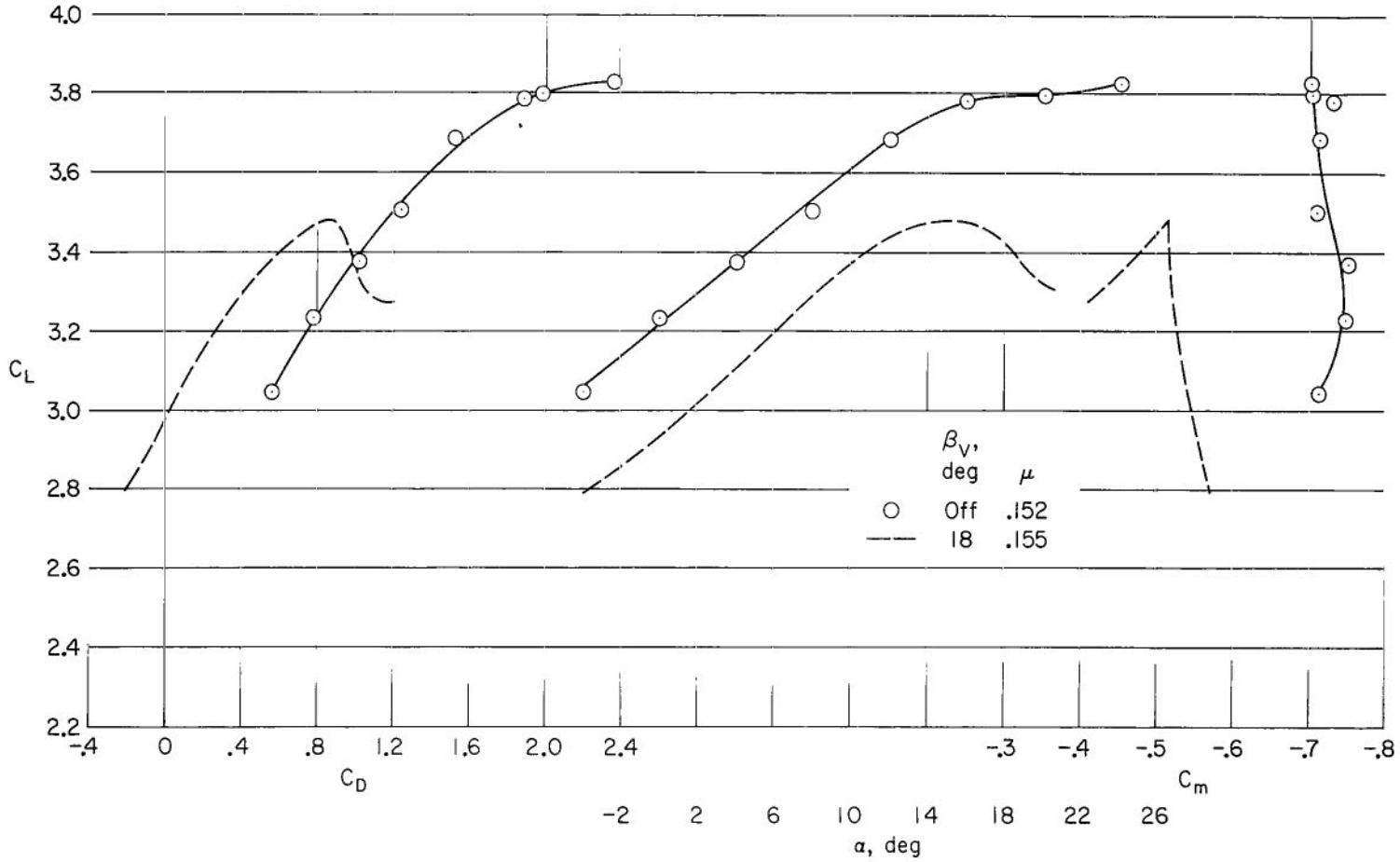

(b) Exit vanes off, $\delta_F = 30°$, $C_{\mu_f} = 0.025$, $V_\infty = 40$ knots.

Figure 13.- Continued.

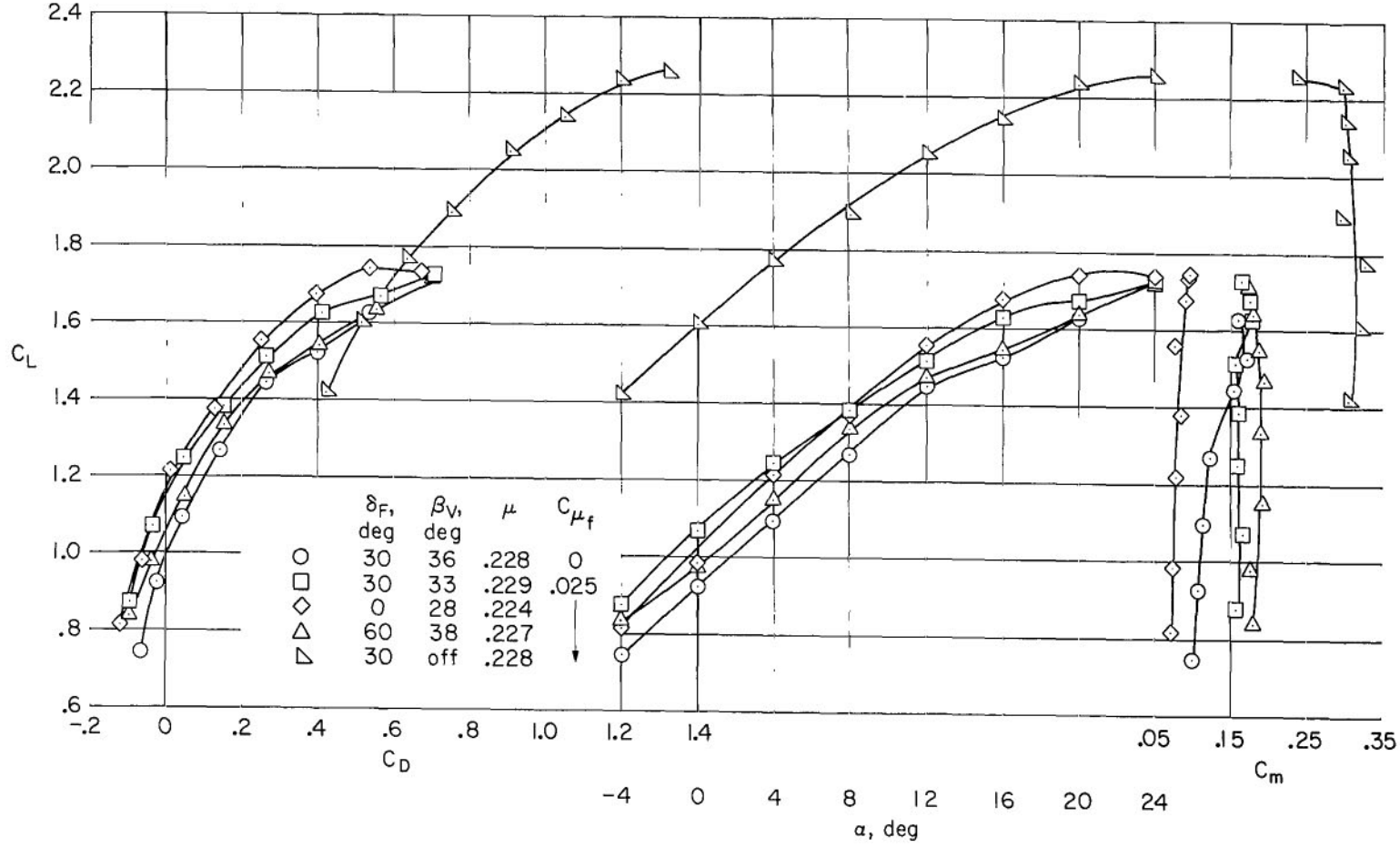

(c) V_∞ = 60 knots.

Figure 13.- Continued.

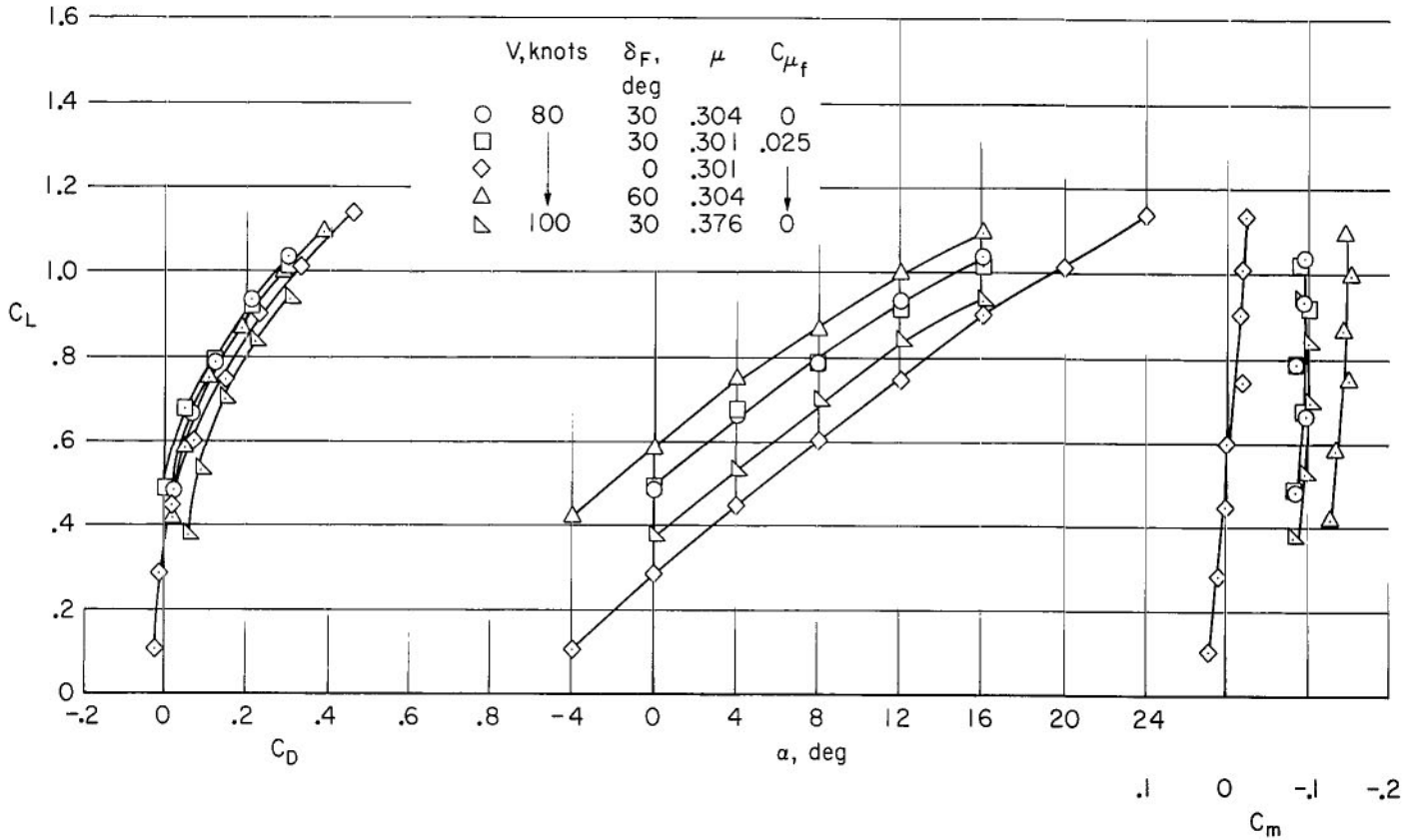

(d) V_∞ = 80 and 100 knots, β_V = 50°.

Figure 13.- Concluded.

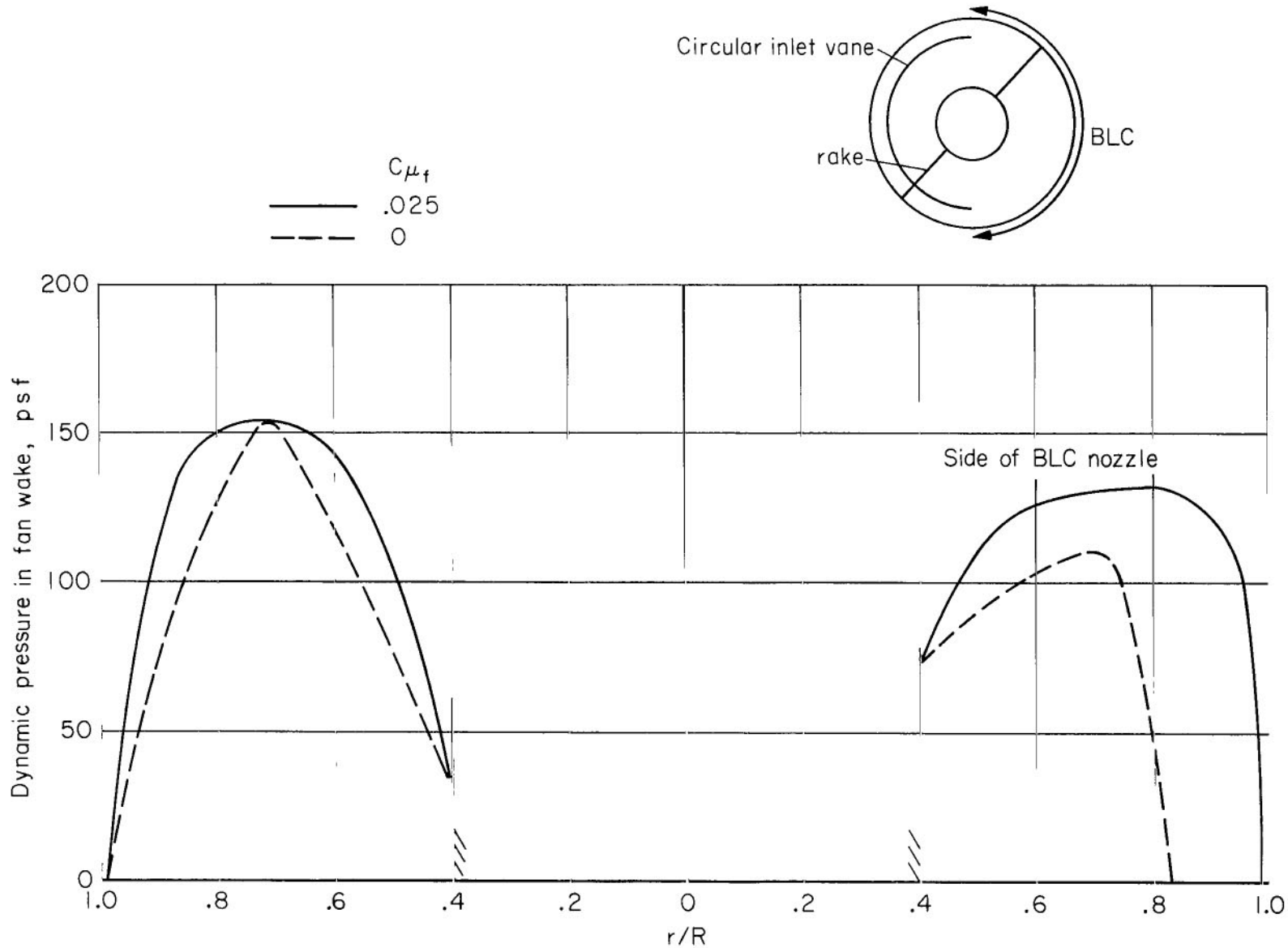

Figure 14.- Effect of BLC on dynamic pressure in fan wake; $V_\infty = 0$, $\beta_v = 0°$, 1700 rpm.

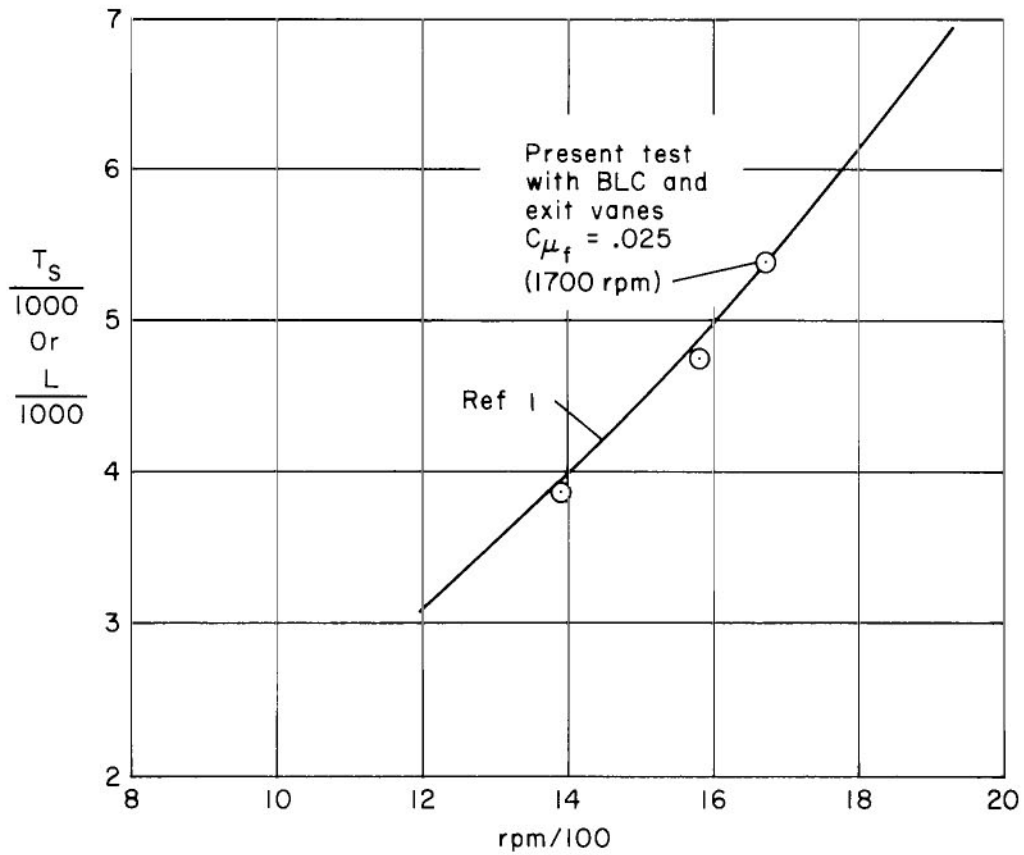

Figure 15.- Comparison of lift of reduced thickness fan with that of the conventional fan; $V_\infty = 0$.

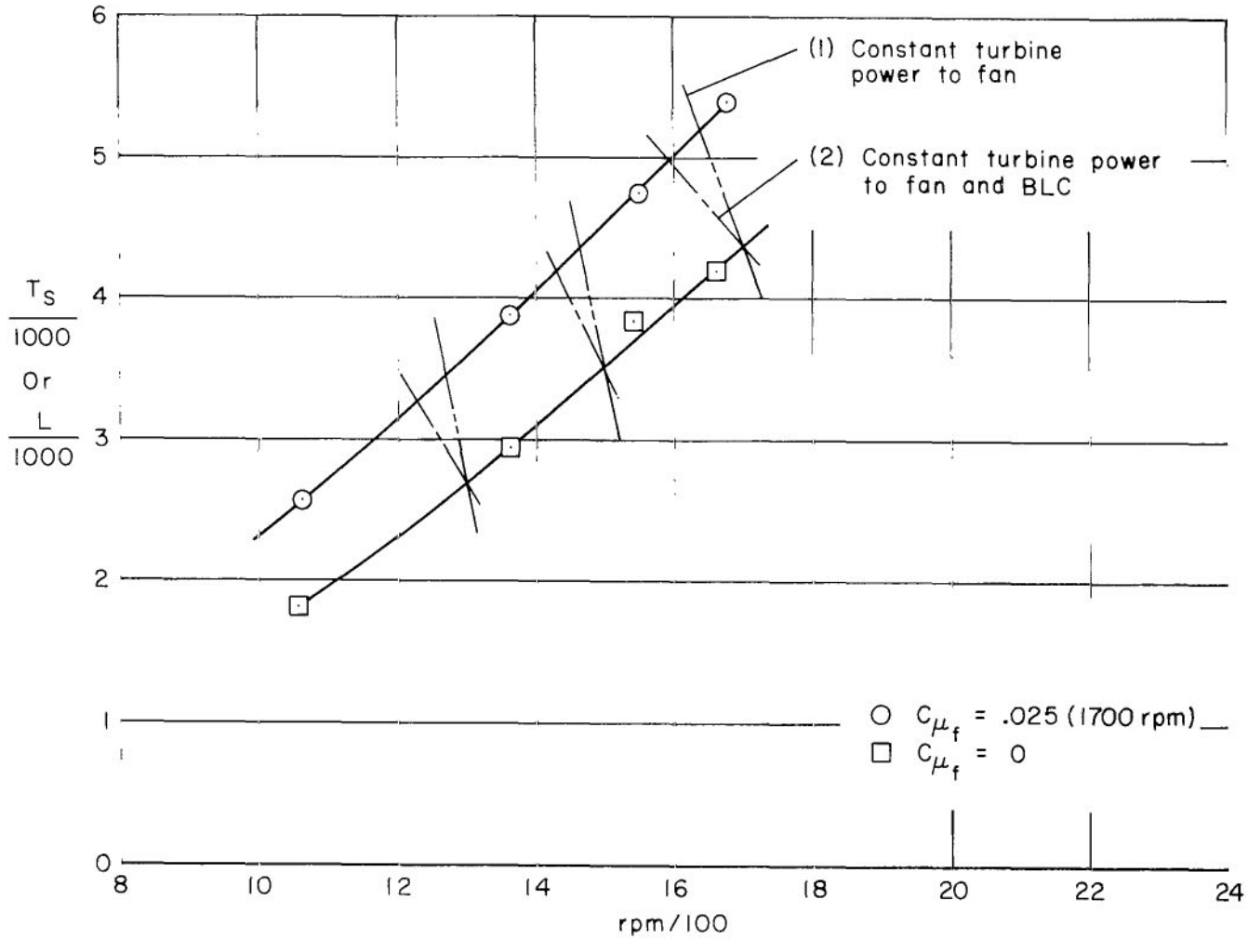

Figure 16.- Effect of boundary-layer control on fan lift; $V_\infty = 0$, $\beta_V = 0°$, constant BLC momentum when in use.

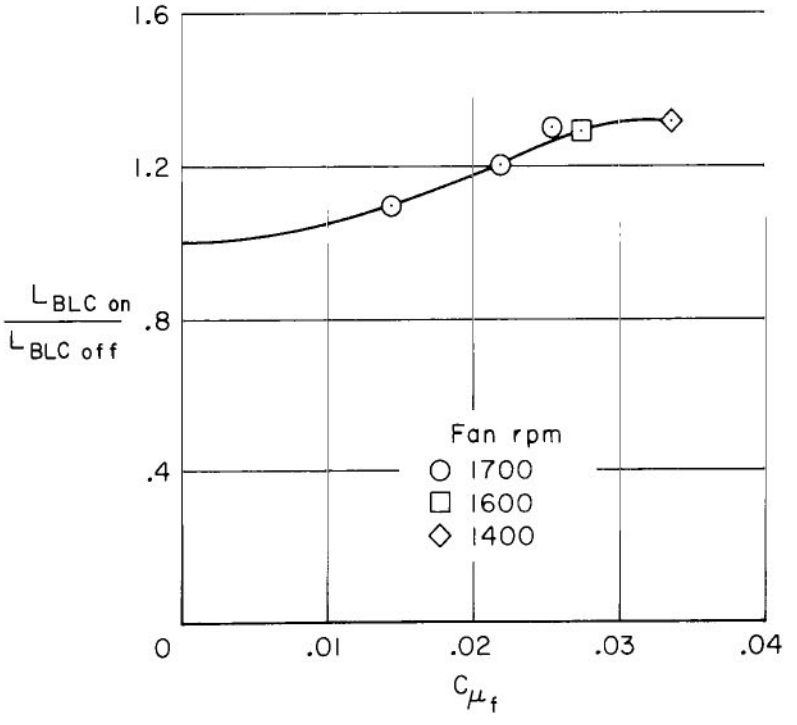

Figure 17.- Variation of fan lift with BLC momentum coefficient; $V_\infty = 0$, $\beta_V = 0°$.

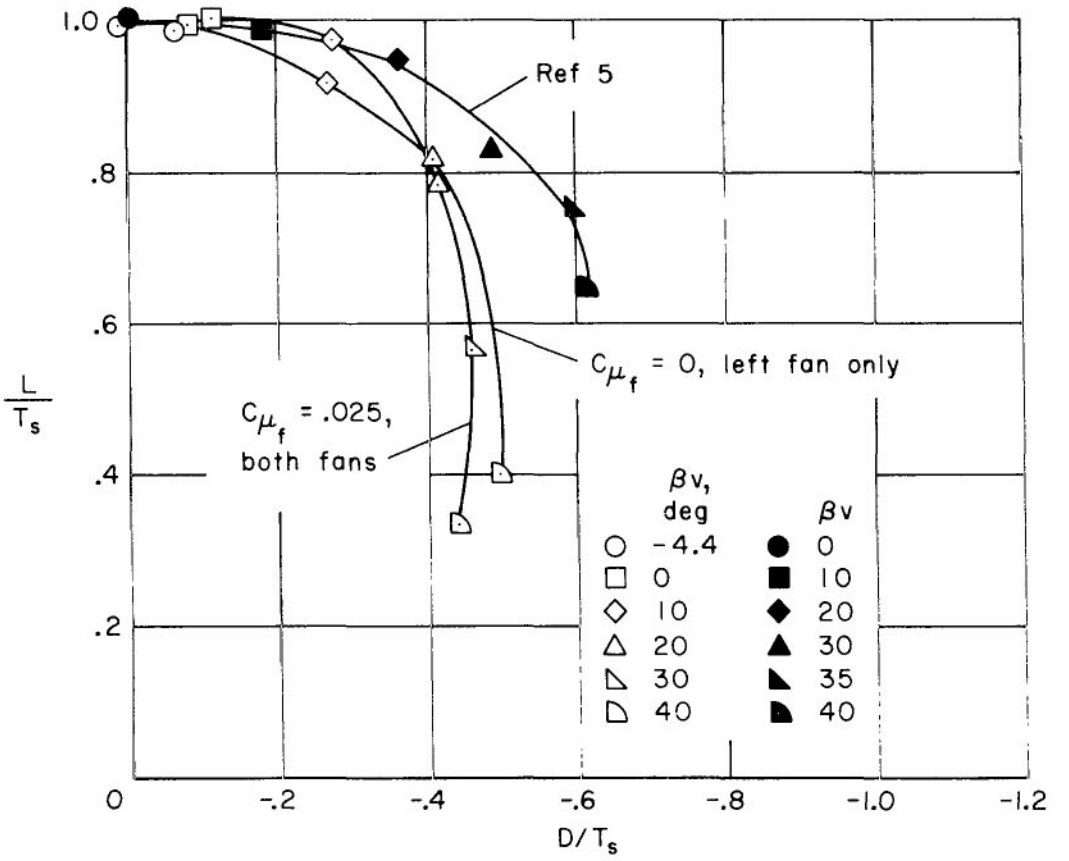

Figure 18.- Exit vane turning effectiveness; V_∞ = 0, 1700 rpm, α = 0°.

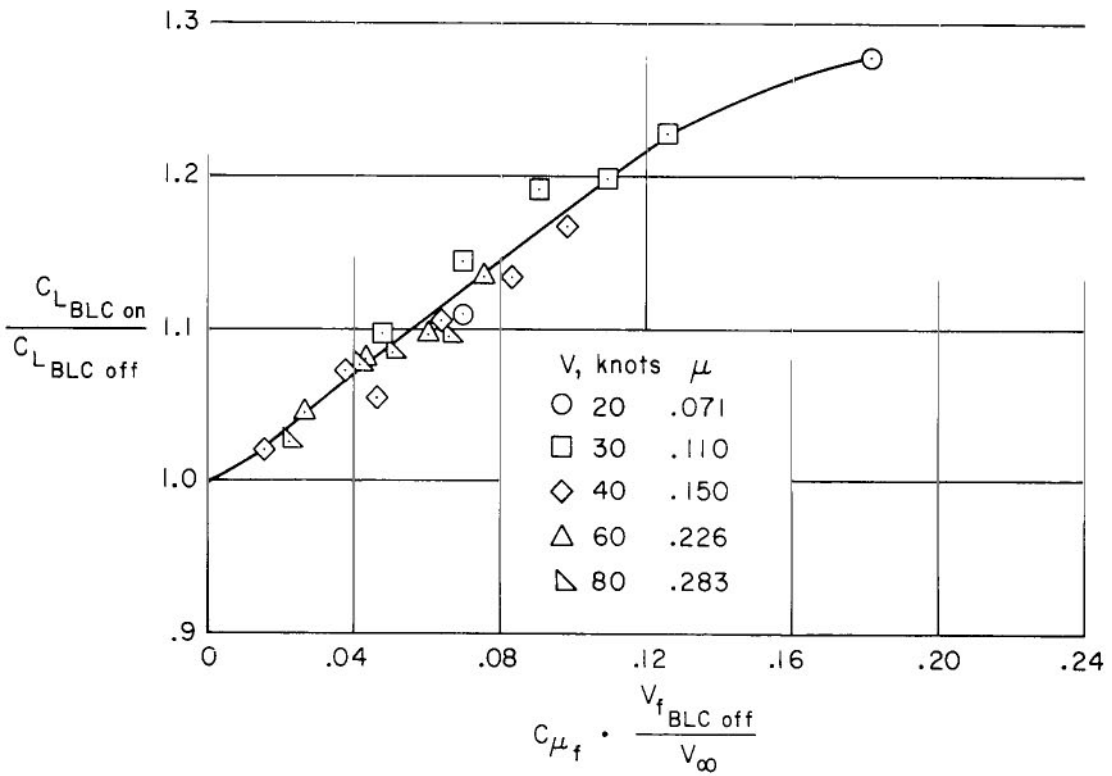

Figure 19.- Correlation of BLC effects on total model lift at several airspeeds; $\beta_v = 0°$, 1700 rpm, $\alpha = 0°$.

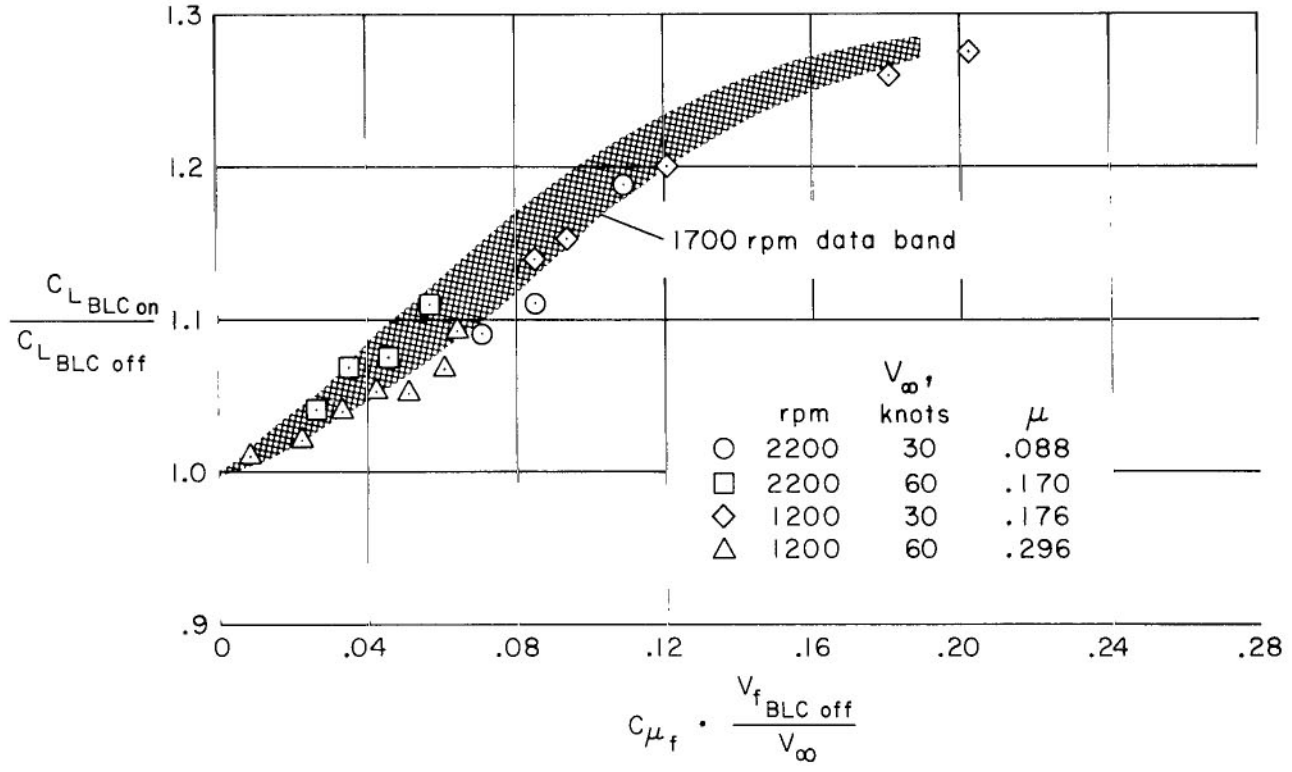

Figure 20.- Correlation of BLC effects on total model lift for several fan speeds and airspeeds; $\beta_v = 0°$, $\alpha = 0°$.

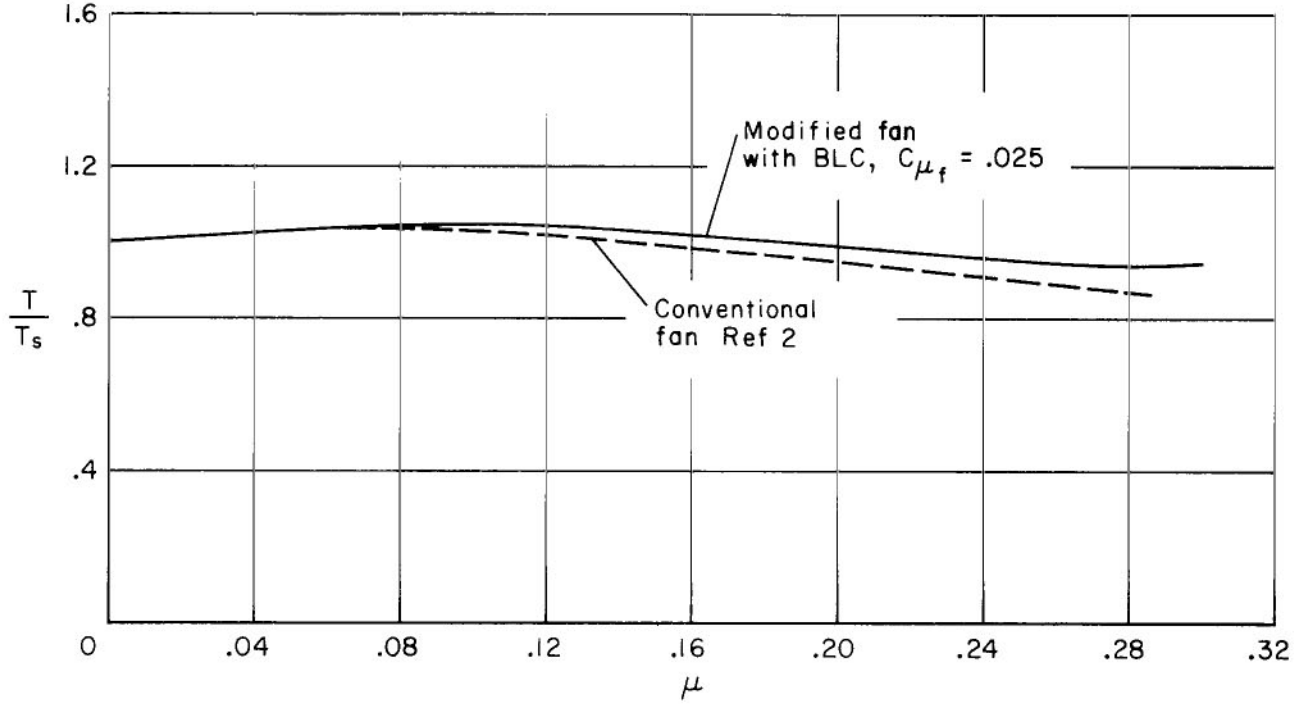

Figure 21.- Comparison of forward speed performance of conventional fan and modified BLC fan; $\beta_v = 0°$, $\alpha = 0°$, 1700 rpm.

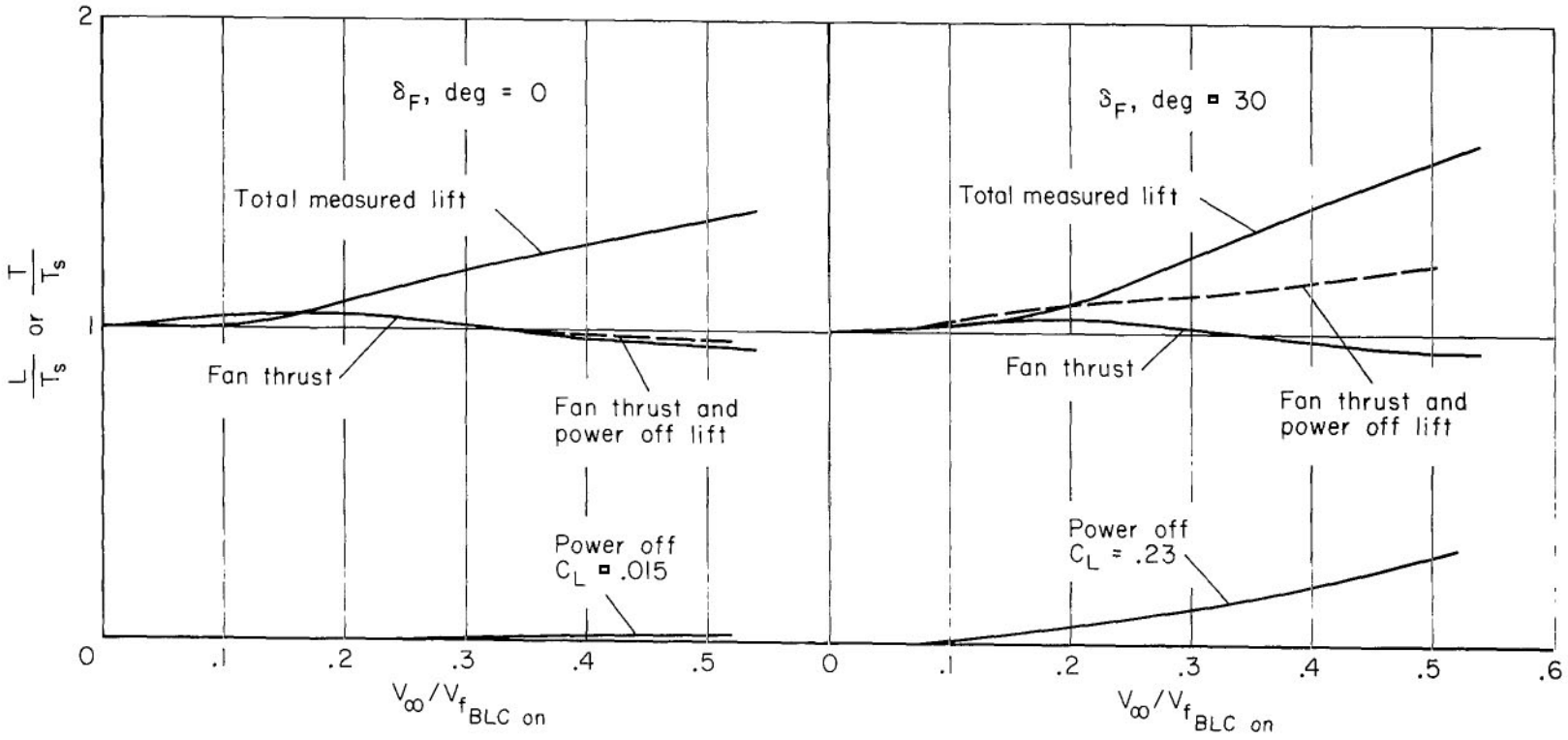

Figure 22.- Effect of fan operation and forward speed on total model lift for two flap deflections; $\alpha = 0°$, 1700 rpm, $\beta_V = 0°$, $C_{\mu_f} = 0.025$.

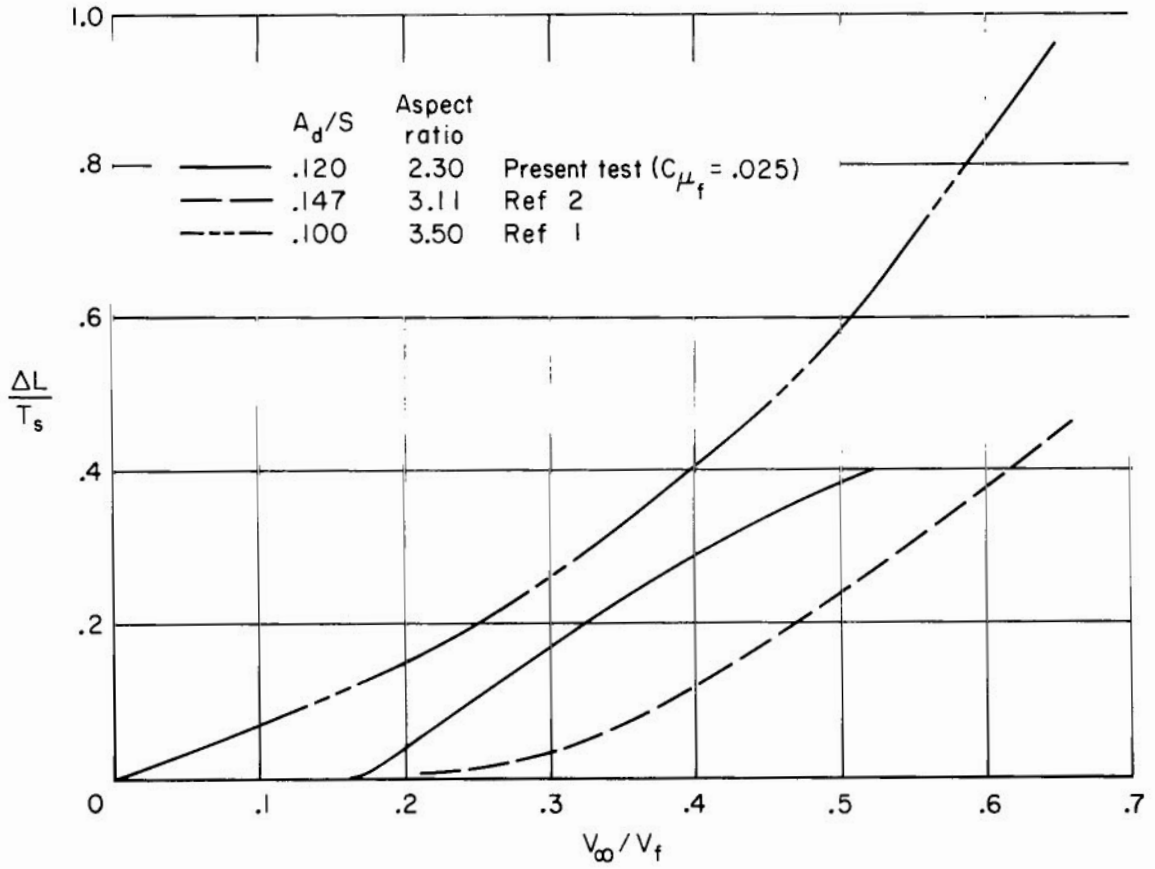

Figure 23.- Comparison of the variation of fan induced lift with airspeed for several fan-in-wing configurations; $\alpha = 0°$, $\beta_V = 0°$, $\delta_F = 0°$.

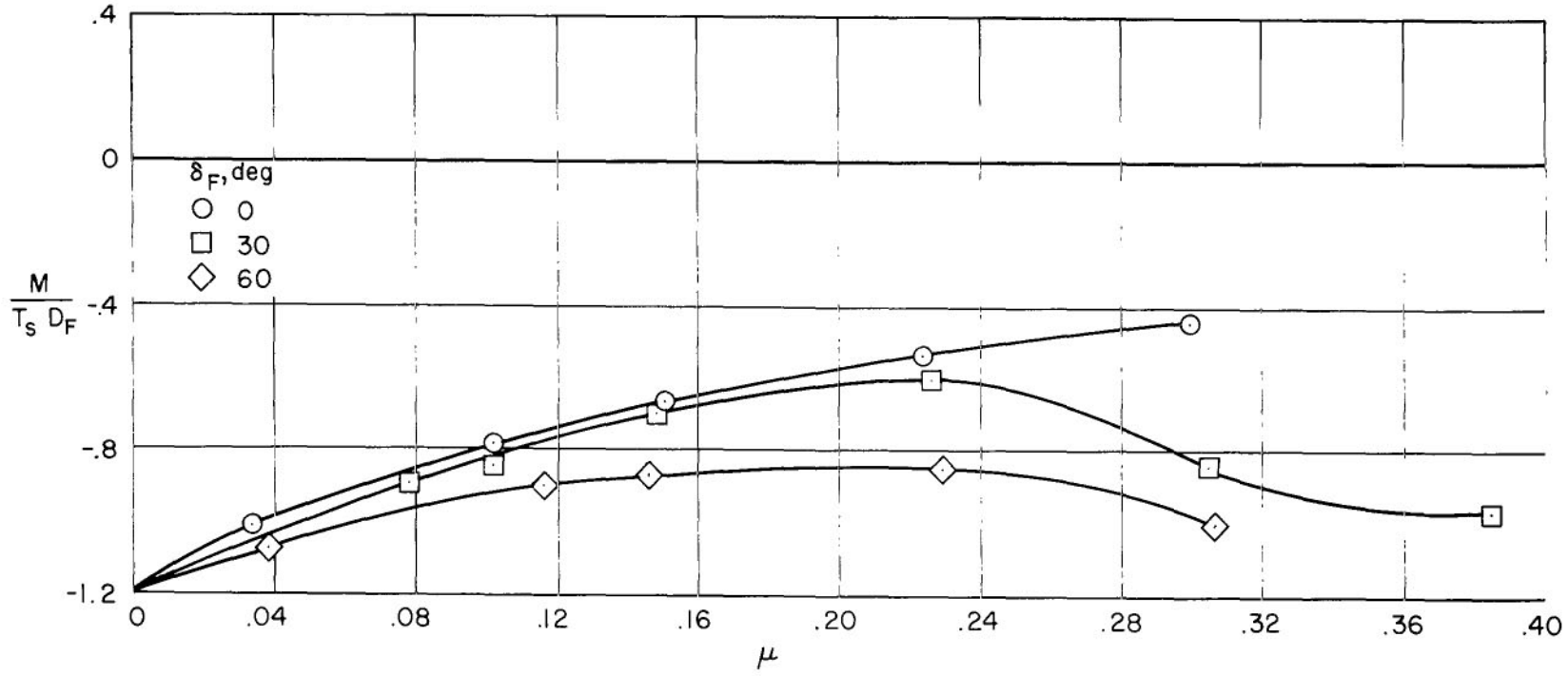

Figure 24.- Variation of pitching moment with tip-speed ratio; 1700 rpm, tail off, $C_{\mu_f} = 0.025$, $\alpha = 0°$, $\beta_v = 0°$.

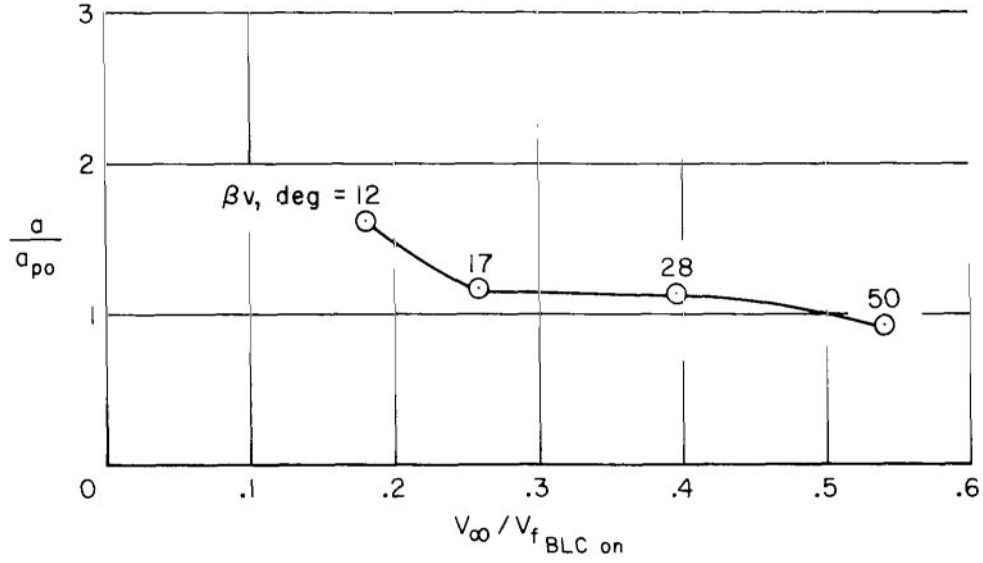

Figure 25.- Effect of lift-fan operation on lift-curve slope; $\delta_F = 0°$, 1700 rpm, $C_{\mu_f} = 0.025$.

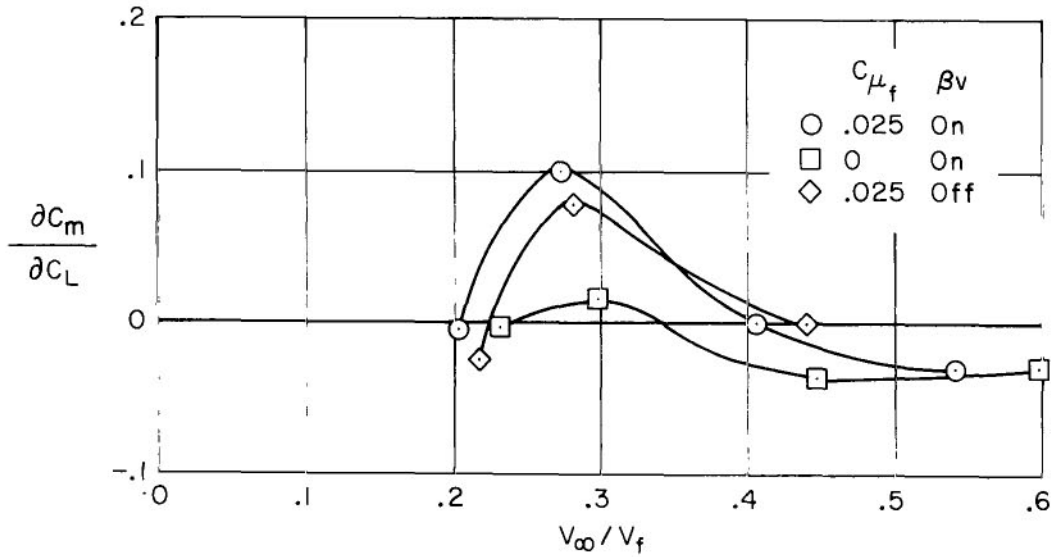

Figure 26.- Variation of static margin with velocity ratio, δ_F = 30°. 1700 rpm.

"The aeronautical and space activities of the United States shall be conducted so as to contribute . . . to the expansion of human knowledge of phenomena in the atmosphere and space. The Administration shall provide for the widest practicable and appropriate dissemination of information concerning its activities and the results thereof."

— NATIONAL AERONAUTICS AND SPACE ACT OF 1958

NASA SCIENTIFIC AND TECHNICAL PUBLICATIONS

TECHNICAL REPORTS: Scientific and technical information considered important, complete, and a lasting contribution to existing knowledge.

TECHNICAL NOTES: Information less broad in scope but nevertheless of importance as a contribution to existing knowledge.

TECHNICAL MEMORANDUMS: Information receiving limited distribution because of preliminary data, security classification, or other reasons.

CONTRACTOR REPORTS: Scientific and technical information generated under a NASA contract or grant and considered an important contribution to existing knowledge.

TECHNICAL TRANSLATIONS: Information published in a foreign language considered to merit NASA distribution in English.

SPECIAL PUBLICATIONS: Information derived from or of value to NASA activities. Publications include conference proceedings, monographs, data compilations, handbooks, sourcebooks, and special bibliographies.

TECHNOLOGY UTILIZATION PUBLICATIONS: Information on technology used by NASA that may be of particular interest in commercial and other non-aerospace applications. Publications include Tech Briefs, Technology Utilization Reports and Notes, and Technology Surveys.

Details on the availability of these publications may be obtained from:

SCIENTIFIC AND TECHNICAL INFORMATION DIVISION

NATIONAL AERONAUTICS AND SPACE ADMINISTRATION

Washington, D.C. 20546